# AN APPLICATION OF PHOTOGRAMMETRIC TECHNIQUES TO THE MEASUREMENT OF HISTORIC PHOTOGRAPHS

by

David A. Strausz, Jr.

A RESEARCH PAPER

submitted to

THE GEOSCIENCES DEPARTMENT

in partial fulfillment of the
requirements for the
degree of

MASTER OF SCIENCE

GEOGRAPHY PROGRAM

June 2001

Directed by
Dr. A. Jon Kimerling

CONTENTS

ILLUSTRATIONS

Figure page

TABLES

Table page

# AN APPLICATION OF PHOTOGRAMMETRIC TECHNIQUES

# TO THE MEASUREMENT OF HISTORIC PHOTOGRAPHS

ABSTRACT: The application of the collinearity solution by resection of the interior and exterior orientation parameters of historical photographs is investigated. The spatial coordinates of seven or more identifiable control points in the field of view of an historical photograph, combined with image coordinates of the control point images, allow solution of all nine unknown orientation parameters. Once the orientation parameters are known, image coordinates of unknown points can be solved by intersection, providing a means for accurate location of those points in space. A form of the collinearity equations is derived that is generally applicable to solutions of terrestrial photograph parameters and the process of solving for the orientation of an historical photograph is demonstrated.

## Introduction

Photography has provided a record of past landscapes over the 150 years since its invention, documenting change due to the natural succession of vegetation, cultural development, environmental evolution, and other inexorable processes, both uniformitarian and catastrophic. These images of past landscapes can be a rich resource for the study of the processes and effects of change in the environment, at least for processes that operate on the time scale of hundreds of years. An effective tool to utilize this resource is the technique of rephotography or repeat photography, in which historic photographs are recreated so that changes in the landscape that have occurred in the intervening time can be readily detected and studied (Figures 1, 2).

Rephotography involves taking a new photograph as closely as possible from the same point in space, with the same camera axis orientation as the original photograph. This can be challenging when, as is often the case, the original camera position and such parameters as camera focal length, or even image format size, if the original negative is not available, are all unknown. Fortunately, much of this information can be derived directly from the geometric properties of the image itself. In addition, it is not necessary for comparative purposes to reproduce the original focal length and image format size, since the same geometric properties will be inherent in any photograph taken from the same point in space with the same orientation.

It is also valuable in the repeated photograph to recreate other environmental parameters of the original photograph, such as season of the year (important for vegetation comparisons) and time of day (affecting shadow length and orientation) so that the new image duplicates as many original parameters as possible making true change in the environment more evident. This is not difficult to do once the spatial orientation of the photograph is established, although recreating

the precise time of day might involve considerable patience. Fortunately, the provenance of much archival photography does record the date of exposure, and further clues can be derived from the geometry of shadows in the image.

There are many advantages to using historic photographs as evidence. The popularity of photography as a recording medium almost since its inception means there is an abundance of images taken for personal, commercial, and scientific purposes that have survived and are available for study. It is a remarkable information source that has not been fully utilized. A valuable characteristic of a photographic image is the immense amount of data that is recorded in the emulsion. At the moment of exposure a permanent record is made of the reflectance values of every object in the field of view. This record exists in great detail as microscopic chemical changes in the emulsion can be resolved to at least 10 microns in the original image scale. The emulsions of even the earliest photographs have this level of resolution, which combined with the large formats common in earlier times, recorded incredibly fine detail. This detail allows researchers to glean information from these images that was unrecognized by the original photographer.

## Rephotography as a Record of Landscape Change

Repeating photography over time has been recognized for over 100 years as a technique to record and study landscape change. Sebastian Finsterwalder pioneered the application of photogrammetric techniques to the measurement of Alpine glaciers as early as 1889 (Hattersley-Smith 1966). The sometimes rapidly changing morphology of glaciers has inspired many researchers to advocate the use of repeated photographs since then. G.K. Gilbert, in the 1899 Harrison expedition to Alaska, made photographs of glaciers with the specific purpose of recording scenes for future comparison. He also repeated in 1903 a glacier photograph in the Sierras taken twenty years earlier (Rogers, Malde, and Turner 1984, 37).

There have since been many studies of landscape change utilizing repeat photography. Rogers, Malde, and Turner (1966) provide a bibliography of over a hundred pages of references collected during their own repeat photography research. Hart and Laycock (1996) have published an updated annotated list of references of studies that have utilized repeat photography for the study of vegetation change, cross referenced by area of study and type of vegetation.

Several examples of these studies are Hastings and Turner (1965), Rogers (1982), and Sallach (1986), documenting landscape change in different habitats of southeast Arizona, the Central Great Basin of Utah, and part of New Mexico, respectively. These studies all utilized historic photographs gleaned from many sources, such as museums and archives, recreated the photos, and used them to deduce environmental changes occurring in the intervening years. In these studies, the only quantitative measurement of change was by Sallach, who covered the photos with a grid to measure relative coverage of different vegetation types.

Several studies have been made to assist in the management of landscapes by investigating the effects of potentially manageable influences, such as fire, disease, grazing, and other human interactions. Two examples are Skovlin and Thomas (1995), and United States Department of Agriculture (1993), which use repeat photography to document changes in the

Blue Mountains of Oregon and the Boise National Forest, respectively. The Blue Mountain study recognized the value of recording the positions of the repeat photographs with the idea of continuing them in the future. Many of these repeat photographs included calibrated stakes in the foreground, which could be used in scale measurements, although most of the comparisons were made through subjective description.

Some studies have used the rich legacy of early photographic coverage of many scenically spectacular areas of the western United States. Happily for posterity, much of the west has inspired considerable photographic coverage since it was first explored, during a time when photographic field techniques, while cumbersome, were well developed. Stevens and Shoemaker (1987) and Webb (1996) are two examples that cover the spectacular landscape of the Colorado River. Stevens and Shoemaker recreated, as a centennial project, many of the photographs taken on the second Powell expedition. Webb organized an expedition to retrace the steps and recreate photographs from the Stanton expedition of 1889-90 as a basis for a study of existing and past ecosystems along the Colorado River. The photographs by Meagher and Houston (1998) of Yellowstone National Park are also in this category. The interest in the park at the turn of the twentieth century led to very extensive photographic coverage which provides many opportunities for repeat photography. The authors have gone one step further in this study by continuing their own earlier repeat photography made in the 1970's into the 1990's. This allowed comparison of change rates across two different time intervals and recorded the change wrought by the large intervening episodic event of the Yellowstone fires of 1988.

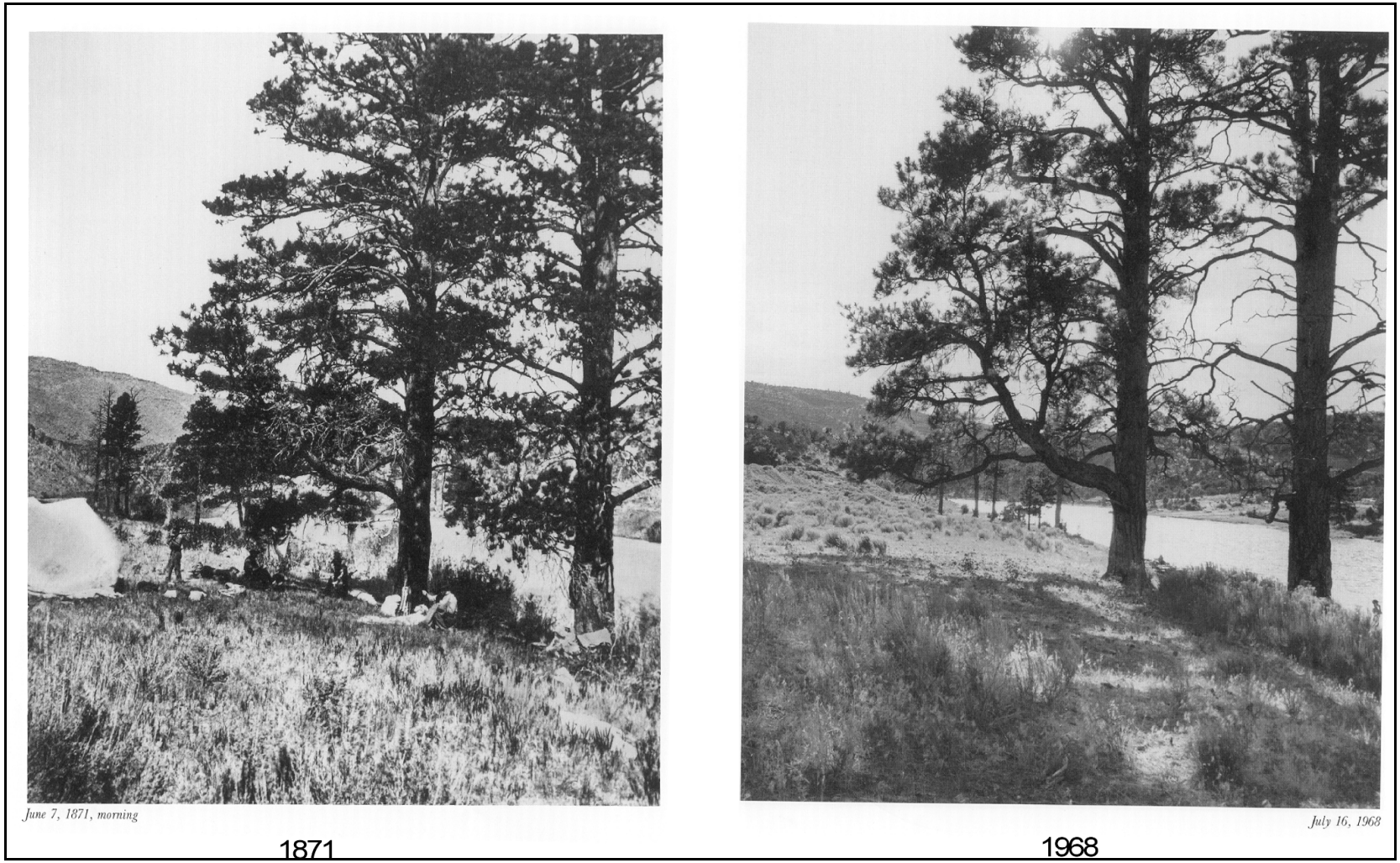


Figure 1. Little Hole campground, from Stephens and Shoemaker.

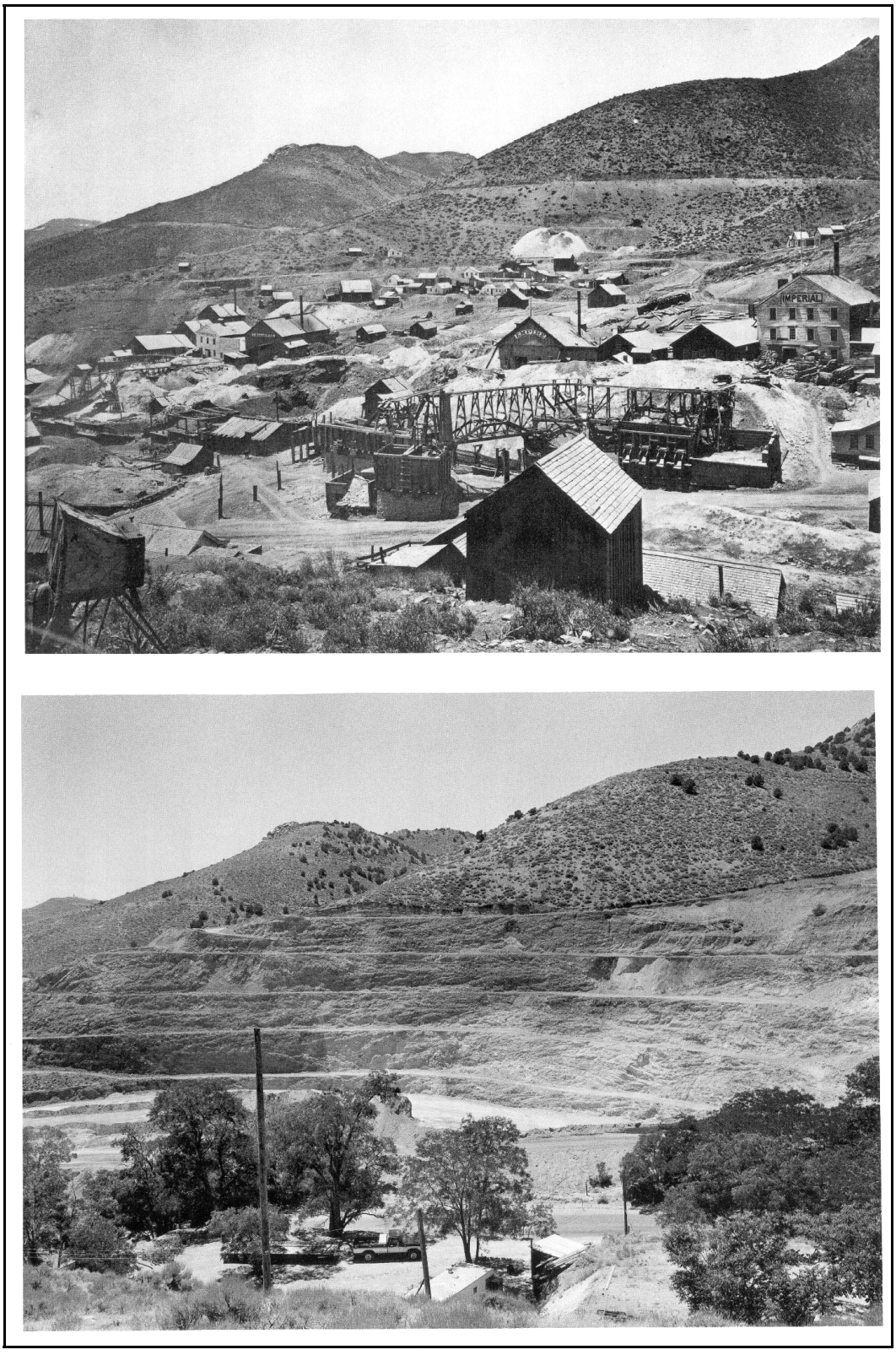


Figure 2. Virginia City, Nevada, 1868 and 1979, from Klett, Manchester, and Verburg

## Techniques

The primary challenge in recreating a photograph is to determine the exterior orientation of the original image, that is, the point in space occupied by the camera (strictly speaking the focal node of the lens) and the orientation in space of the image (emulsion) plane. Note that the focal length is not strictly necessary to this orientation since any image taken from the same perspective point in space, at the same orientation, will be identical to any other image with the same exterior orientation, as long as they are scaled identically and cropped to the same field of view. The usefulness of the repeat photography directly depends upon the accuracy of the recreation of the original, particularly if the images are to be compared in a quantitative manner. If an area of interest exists in the near foreground of the photos, a slight change in orientation can significantly change the proportions in the respective fields of view (Harrison 1974, 471). Some studies have only been concerned with approximating the camera position, which limits their comparisons to subjective analysis (Goin 1992).

Several methods have been used to reproduce the original image orientation. By far the simplest and most often used, judging from the studies reviewed, is to merely move the camera position (or initially, the eyeball of the photographer) around until the image in the viewfinder or on the ground glass at the image plane matches that of the original image. A further step in sophistication is to compare actual measurements of parallax between identifiable objects in both images. This method has been applied as an iterative process, where after a photograph is taken measurements between objects in the image are compared to the original; any differences indicate needed changes in the orientation. A third method, common to terrestrial photogrammetric applications, is to plot lines from objects that lie on lines of intersection with the camera station on a plan view. To locate the camera station by the intersection of such lines is only possible when the image contains a very rich field of identifiable objects (Borchers (1977, 16). Another method, proposed in this paper, is to subject measurements of the original image to photogrammetric analysis, in order to directly solve for the exterior orientation.

The trial and error, "eyeball," method has certainly been the most popular, probably because of its simplicity, but can still involve hours of moving about in search of the illusive point of perspective (U.S. Department of Agriculture 1993, 48). This method can yield very accurate results for images that contain a good mix of identifiable objects throughout the depth of field of the view, and particularly when objects are lined up in one or two ranges that define unique lines terminating at the point of perspective, a condition which is not often encountered. In the above conditions, once near the original perspective point, deviations of only a few centimeters may be readily perceived. This process can be systematized by first lining up with objects along the original image center line, then moving in and out along the center line until the parallax of objects to either side match (Malde 1973, 198).

The method proposed by Harrison (1974) and clearly explained and applied by Klett, Manchester, and Verburg (1984) is a considerable improvement in terms of accuracy and repeatability. Harrison points out that there are six unknown elements of the orientation of the original image: three coordinates in three dimensional space to define the camera position, and three angular displacements about three orthogonal axes of the image plane. These unknown elements can be reconstructed theoretically by comparing six or more independent

measurements. Harrison uses the measurements of image distances between identifiable points. To satisfy the requirement for at least six independent measurements, at least five points are needed (since independent lengths between n points equals 2n-3). To remove the element of scale between photos, the distances can be normalized by dividing all measurements in each photo by a common measurement in the respective photo. If both photos have the same exterior orientation, all normalized measurements will be the same.

Harrison further recommends constructing axes in the photos perpendicular to one of the photo distances. This is exemplified in Figure 3, with EE' perpendicular to the distance AB, and lines CC' and DD' perpendicular to EE'. In this way the ratios between the line segments created by the perpendicular axes provide a quantifiable measurement of the relative parallax of different objects, which can be readily compared between photos. If the axes are constructed approximately perpendicular and parallel to the image horizon, the differences in the ratios between photos can clearly indicate what relative movement is necessary.


36. Timothy O'Sullivan, 1867. Rock formations, Pyramid Lake, Nev. (Massachusetts Institute of Technology.)


37. Mark Klett for the Rephotographic Survey Project, 1979. Pyramid Isle, Pyramid Lake, Nev.

Figure 3. Pyramid Lake, Nevada, from Klett, Manchester, and Verburg.

## Analytical Orientation Solution

Analytical photogrammetry is the application of mathematical principles to measurements in photographic image planes in order to model and reconstruct both the original spatial orientation of the image and the relative and absolute locations of imaged object points. While the principles of spatial geometry basic to analytical photogrammetry were seriously investigated as early as the 15th century by such polymaths as Leonardo da Vinci and Albrecht Durer, their application to the measurement of photographs largely began with the work of Sebastian Finsterwalder at the beginning of the twentieth century. The development of analog measuring devices that recreated the geometry of aerial photographs for the purposes of topographic mapping dominated the practical application of photogrammetry for the first half of the twentieth century. The solution of the same problems analytically requires an amount of computation that precluded practical application before the advent of computer processing. Otto von Gruber, who derived the projective equations fundamental to modern analytical photogrammetry, is famously quoted as saying that their application was "a waste of time and is of minor importance." (Thompson 1966, 461-64).

In photogrammetry the orientation of an image is defined by several parameters. The interior orientation elements are the focal length of the camera, which is the perpendicular distance from the film plane to the focal node of the lens, and the location on the image where that perpendicular line intersects the image plane, called the Principal Point (PP in Figure 4). Knowledge of these parameters is important if the image is to be used for photogrammetric measurements. In a non-metric camera, defined as any camera not specifically designed for photogrammetry (Atkinson 1980, 64), the interior parameters are not necessarily known with any precision (Faig 1976, Karara 1972) . This is certainly the case for nearly all historic photographs. The exterior orientation is defined by six parameters, the three spatial coordinates of the camera station and three angular measurements that define the spatial orientation of the image plane. In the United States it is conventional to use the terms $\omega$, $\phi$, and $\kappa$ to indicate the rotation around respectively and in order, the x, y, and z axes of an orthogonal coordinate system parallel to the space coordinate system in use in order to transform a plane parallel to the x, y axes of the space coordinate system into a plane parallel to the image plane. These rotations are considered to be positive in a right-handed sense relative to their respective axes (Figure A1). These six parameters of exterior orientation need to be known to recreate an historic photograph.

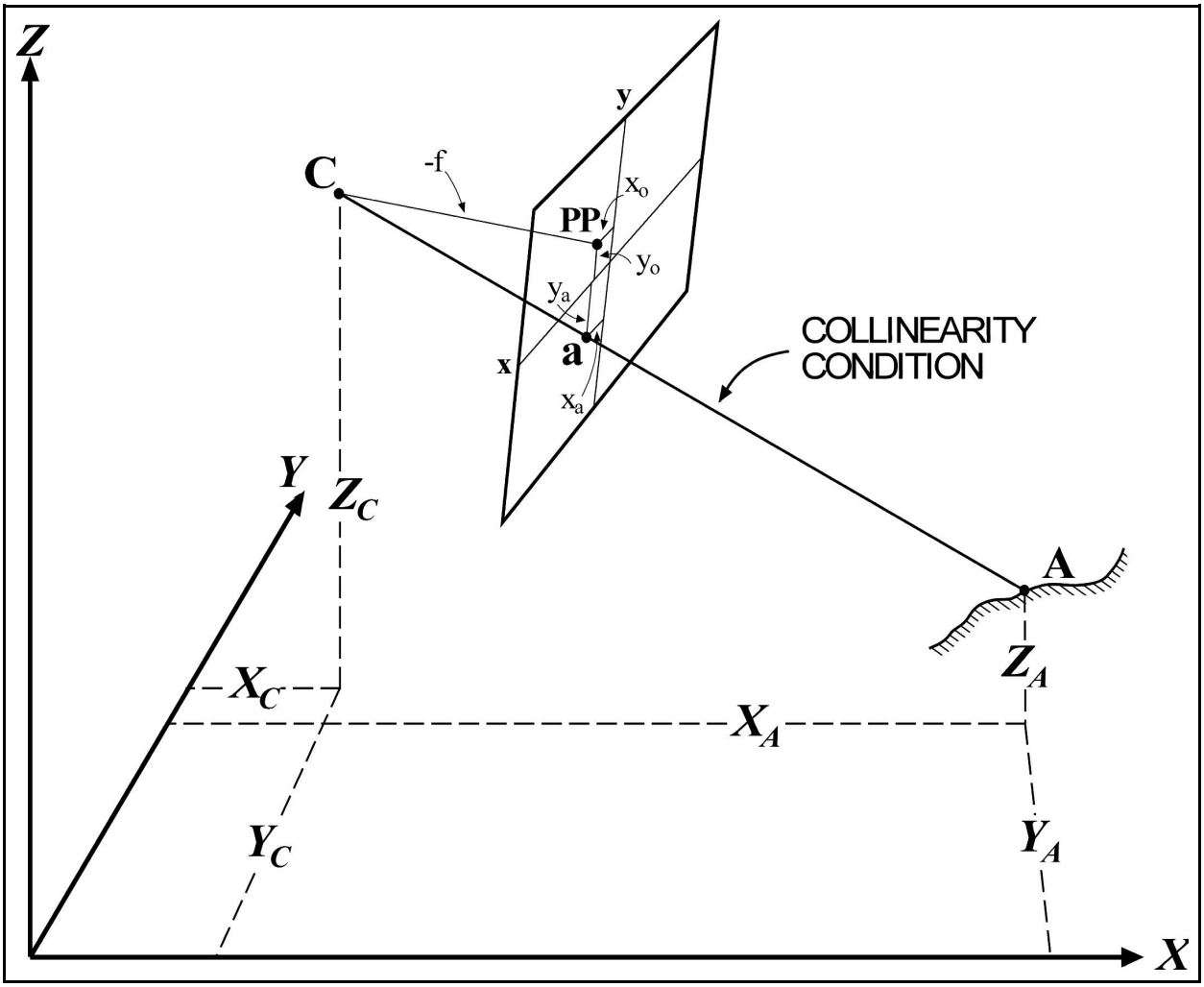


Figure 4. The Collinearity Condition, C, a, and A lie on a straight line.

The basic problem in analytical photogrammetry is to mathematically relate the positions in space of imaged objects to the positions of their image points in the plane of the image, and vice versa. The most basic geometric concept utilized in developing solutions to this problem is the collinearity condition which is that the camera station, the image point, and the imaged object all lie on a straight line (Figure 4). This concept is used to develop the collinearity equations, usually in the form where the image coordinates of an object are expressed as functions of the interior orientation parameters, the exterior orientation parameters, and the space coordinates of the object. These equations are derived in Appendix A and shown below:

$$x_a = x_o - f\left[\frac{m_{11}(X_A - X_C) + m_{12}(Y_A - Y_C) + m_{13}(Z_A - Z_C)}{m_{31}(X_A - X_C) + m_{32}(Y_A - Y_C) + m_{33}(Z_A - Z_C)}\right] \quad (1)$$

$$y_a = y_o - f\left[\frac{m_{21}(X_A - X_C) + m_{22}(Y_A - Y_C) + m_{23}(Z_A - Z_C)}{m_{31}(X_A - X_C) + m_{32}(Y_A - Y_C) + m_{33}(Z_A - Z_C)}\right] \quad (2)$$

In these equations $x_a, y_a$ are an object $A$'s image coordinates; $X_A$, $Y_A$, $Z_A$ are the object's coordinates in object space; $X_C$, $Y_C$, $Z_C$ are the object space coordinates of the camera position; $m_{11}$-$m_{33}$ are the coefficients of the orthogonal transformation between the image plane orientation and object space orientation, and are functions of the rotation angles $\omega$, $\phi$, and $\kappa$; $x_o$, $y_o$, and $f$ are the interior orientation parameters of the image, the image coordinates of the photo principal point and the camera focal length, respectively.

In the conventional situation where the elements of interior orientation are known the collinearity equations can be used to solve for the six unknown elements of exterior orientation by developing two equations for each of at least three control points of known location. Since these equations are non-linear they are first linearized by the use of a Taylor series expansion of the function with respect to each of the unknown elements. This results in a linear function of the general form, for equation (1):

$$\begin{aligned} x_a - F_O = {} & \left(\frac{\partial F}{\partial \omega}\right)_O \Delta\omega + \left(\frac{\partial F}{\partial \phi}\right)_O \Delta\phi + \left(\frac{\partial F}{\partial \kappa}\right)_O \Delta\kappa + \left(\frac{\partial F}{\partial X_C}\right)_O \Delta X_C \\ & + \left(\frac{\partial F}{\partial Y_C}\right)_O \Delta Y_C + \left(\frac{\partial F}{\partial Z_C}\right)_O \Delta Z_C = 0 \end{aligned} \quad (3)$$

where $F_O$ is the evaluation of the original function $F$ with estimated values of the unknowns, the coefficients of the form $\left(\frac{\partial F}{\partial a}\right)_O$ are partial derivatives of $F$ relative to the unknown elements *"a"* and evaluated using original estimates of the unknowns, and the $\Delta a$*'s* are corrections to the original estimated values for unknowns "*a*"and which are solved for as unknowns for the combination of linear equations. The solution moves through several iterations, applying the resulting corrections from each iteration to the previous estimates, running until the corrections, hopefully, approach zero (Burnside 1985, 331-34; Gullberg 1997, 767). This approach also usually incorporates an unknown variance factor in the linear functions, so that in the case where more equations can be developed than there are unknowns, a least squares solution can be performed, by first normalizing the system of equations, to solve for a best fit with the given measured control point coordinates.

Several reduction methods have been developed to deal specifically with the non-metric camera situation, where the interior orientation is unknown (Karara 1979, 35-38; Atkinson 1980, 64-72; Faig 1975; Bopp and Krauss 1978). The Direct Linear Transformation of Abdel-Aziz and Karara (1971, 1974) provides a direct transformation between measured image coordinates and

object space coordinates, bypassing entirely the interior and exterior orientation elements of the image. While these methods have advantages of computational efficiency when used for photogrammetric measurements using non-metric cameras in general, they do not directly address recovering the exterior orientation elements that are needed for rephotography.

In adapting the collinearity solution to the situation of recovering the original orientation of historical photographs, it is necessary to add to the linearized equations terms for the additional unknowns of the original interior orientation, $x_o$, $y_o$, and $f$. This results in the following linear versions of equations (1) and (2) (derived in Appendix B):

$$\begin{aligned} x_a - F_O + v_{x_a} &= d_{11}\Delta\omega + d_{12}\Delta\phi + d_{13}\Delta\kappa + d_{14}\Delta X_C + d_{15}\Delta Y_C + d_{16}\Delta Z_C \\ &\quad + d_{17}\Delta x_o + d_{18}\Delta y_o + d_{19}\Delta f \end{aligned} \tag{4}$$

$$\begin{aligned} y_a - G_O + v_{y_a} &= d_{21}\Delta\omega + d_{22}\Delta\phi + d_{23}\Delta\kappa + d_{24}\Delta X_C + d_{25}\Delta Y_C + d_{26}\Delta Z_C \\ &\quad + d_{27}\Delta x_o + d_{28}\Delta y_o + d_{29}\Delta f \end{aligned} \tag{5}$$

These equations use the shorthand notation of $d_{ab}$ to indicate the partial derivatives of the original equations for the respective unknowns. In addition, a variance term $v$ has been added to allow the least squares solution when there are more equations than unknowns. (In the situation of a unique solution, the $v$ terms become zero.)

A system of linear equations based on the development of (4) and (5) for our nine unknowns based on $n$ control points can be described in matrix notation as follows:

$$_{2n}\boldsymbol{L}^{1} + {}_{2n}\boldsymbol{V}^{1} = {}_{2n}\boldsymbol{D}^{9}{}_{9}\boldsymbol{X}^{1} \tag{6}$$

where $\boldsymbol{L}$ is the matrix of the values of differences between calculated and measured image coordinates ($x_a$ - $F_O$ and $y_a$ - $G_O$), $\boldsymbol{V}$ is the matrix of variances, $\boldsymbol{D}$ is the matrix of the partial derivative coefficients, and $\boldsymbol{X}$ is the matrix of corrections to the estimated unknown values. It can be demonstrated that the nine normal equations necessary for a least squares solution can be expressed as (Wolf 2000, 510-12; Thompson 1966, 57-59):

$$(\boldsymbol{D}^T\boldsymbol{D})\boldsymbol{X} = \boldsymbol{D}^T\boldsymbol{L} \tag{7}$$

where $\boldsymbol{D}^T$ is the transpose of matrix $\boldsymbol{D}$. Solving for $\boldsymbol{X}$ yields:

$$\boldsymbol{X} = (\boldsymbol{D}^T\boldsymbol{D})^{-1}(\boldsymbol{D}^T\boldsymbol{L}) \tag{8}$$

with $(\boldsymbol{D}^T\boldsymbol{D})^{-1}$ indicating the inverse of matrix $(\boldsymbol{D}^T\boldsymbol{D})$.

Initial estimates are made of all of the nine unknown elements, which are used to calculate the elements of matrices $\boldsymbol{D}$ and $\boldsymbol{L}$ in equation (8), which is then solved for the $\boldsymbol{X}$ matrix, which gives the corrections to apply to the initial estimated values. This process is iterated, using the corrected estimate values from each successive iteration, continuing until the correction values approach zero. The process of estimating the initial values is important, since values

differing too greatly from actual could lead to a divergent solution. Dewitt has proposed a method of computing initial values addressing the often difficult visualization of orientation angles in terrestrial photography. It is anticipated that estimates of sufficient accuracy may be made from empirical inspection of the image and initial location of the camera station.

The described solution assumes that measurements on the image accurately represent true positions on the focal plane of the image at the time of exposure. This is almost surely not strictly the case. Factors that could affect the accuracy of these points include departure from true flatness of the emulsion at exposure, subsequent distortion of the emulsion, and lens distortions. Further disruption to the collinearity situation results from atmospheric distortion and the departure caused by the curvature of the earth in three dimensional space versus that modeled by the space coordinate system in use. While not addressed in this project, it should be understood that all of these factors could be modeled and added as corrections to the $x_a$, $y_a$ image coordinates in the collinearity equations. These can be treated as additional unknown elements which can be solved for, given a sufficient number of control points.

Karara and Abdel-Aziz (1974) have demonstrated that for a wide range of non-metric cameras (including a Kodak Instamatic!) unless very high precision is needed, most of the corrections to image coordinate measurements may be ignored. Therefore, for this demonstration, the measurements from the photographs will be used without correction.

## Demonstration

A photograph from the Benjamin Gifford collection in the Oregon State University Archives was chosen to demonstrate the application of photogrammety to a historic photograph. The chosen photograph was taken sometime ca. 1915-1920 and depicts the Shepperd's Dell Bridge on the Columbia River Highway in the western Columbia River Gorge of Oregon (Figure 5). This photograph contains images of points, particularly on the bridge structure, which can be identified and located today relatively easily.


Figure 5. Shepperd's Dell Bridge, from the Benjamin Gifford collection, Oregon State University Archives

Seven points were located in the field of view of the original image that were subsequently located in the current landscape and measured with some precision as to their positions in space. This was done by first setting three base survey points, located relative to each other by triangulation and distance measurement using a Nikon DTM-A20LG total station, off of the east end of Shepperd's Dell bridge (points A, B, C in Figure 6). Then the positions in space of the control points were located by triangulation from the base points, using the theodolite function of the total station. This allowed measurement of the control points remotely, without having to physically occupy the points. The total station field measurements are tabulated in Appendix D.

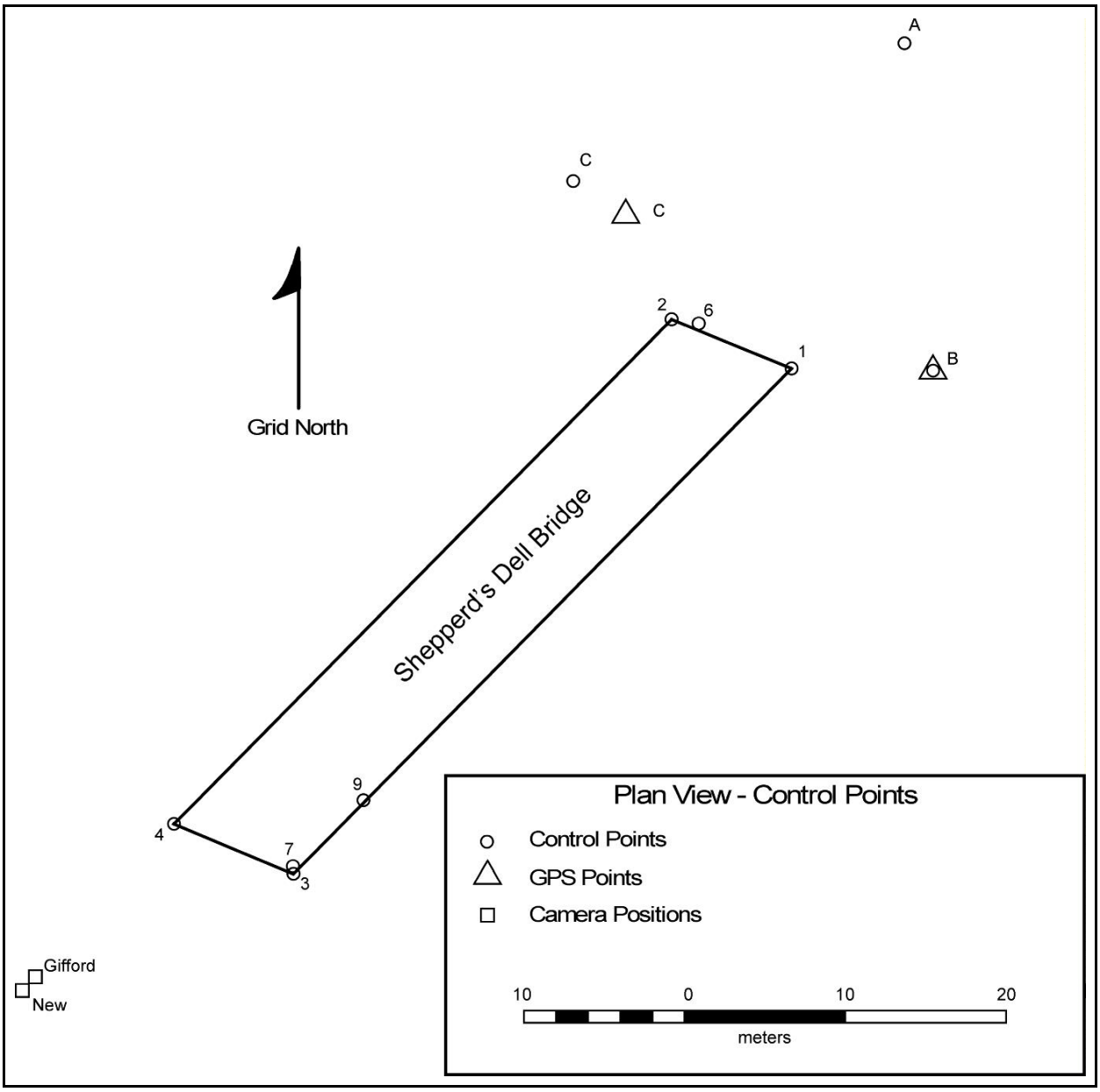


Figure 6. Plan view of control points

In order to tie the base survey points into a general reference system (UTM zone 10, NAD 1983), their positions were measured by occupying them for about 5 minutes each with a Trimble GeoExplorer II code-phase GPS receiver. On the day of observations, constellation and terrain geometry limited solutions to points B and C. The raw GPS data were reduced with Trimble software by postprocessing to differentially correct the observations. The reduced data points were generally distributed about the mean for each point within about 5 meters,with several outliers as much as 20 meters from the mean (Figure 7). These results are consistent with the precision expected with this type of receiver. The horizontal distance BC calculated from mean

GPS positions was about 5 meters less than the distance measured by total station. Therefore, the local coordinate system was tied only to the mean GPS position of point B, and the grid azimuth from A to B was set at 174°, which was calculated from the grid azimuth between the GPS positions of B and C. This results in a local coordinate system which only approximates true UTM coordinates. The field data were then reduced to express the control point locations in this local coordinate system (Table 1).

Table 1. Control point spatial coordinates

| point | E | N | Z | point | E | N | Z |
|---|---|---|---|---|---|---|---|
| A | 646.181 | 4025.567 | 50.901 | 3 | 608.17 | 3973.78 | 52.79 |
| B | 647.967 | 4005.151 | 53.988 | 4 | 600.74 | 3976.90 | 52.72 |
| C | 625.579 | 4016.985 | 55.767 | 6 | 633.38 | 4008.09 | 51.32 |
| 1 | 639.16 | 4005.30 | 52.78 | 7 | 608.14 | 3974.27 | 50.98 |
| 2 | 631.70 | 4008.36 | 52.79 | 9 | 612.52 | 3978.38 | 51.68 |

Note: Coordinates are meters in local coordinates approximately equal to UTM zone 10, NAD 83. Z is meters MSL. Add 562000m to E and 5040000m to N coordinates.

Control point descriptions:

| | |
|---|---|
| A | N road shoulder, E of NE end of bridge |
| B | Top of Rock, SE of NE end of bridge |
| C | Top of Rock, N of NE end of bridge |
| 1 | Apex, SE pillar of bridge |
| 2 | Apex, NE pillar of bridge |
| 3 | Apex, SW pillar of bridge |
| 4 | Apex, NW pillar of bridge |
| 6 | Bottom SE corner of NE pillar, intersection with sidewalk |
| 7 | Bottom NE corner of SW pillar, intersection with sidewalk |
| 9 | Center of ridge (N face) on column, near column top, 20th column from W pillar, S rail of bridge |

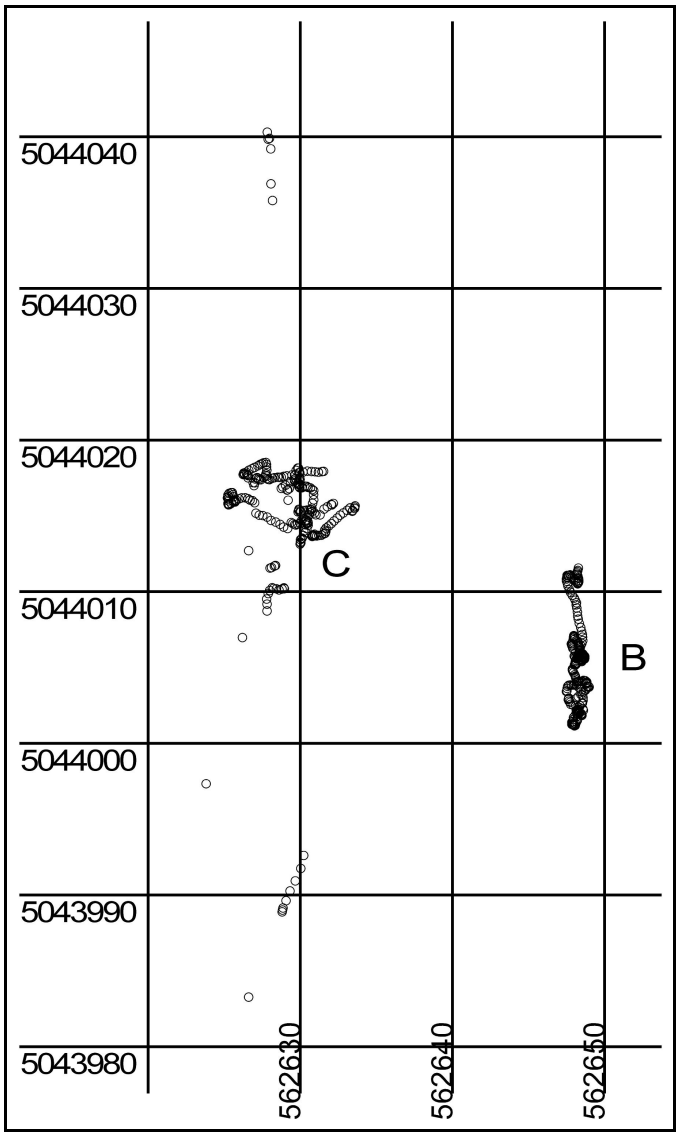


Figure 7. GPS positions, points B and C

The original Gifford photograph was represented by a 6.5x8.5 inch glass positive, which presumably was contact printed from the original negative. This plate was digitized using a flat bed scanner at a resolution of 300 pixels per inch. This digitized image was then measured using Macromedia Freehand software. All measurements were referenced to a coordinate system parallel to the the scan grid with an origin at the lower left corner of the image. The resulting control point image locations are tabulated in Table 2.

Table 2. Control point image coordinates

| | Gifford Photo | | New Photo | |
|---|---|---|---|---|
| point | x | y | x | y |
| 1 | 109.745 | 54.550 | 80.305 | 39.766 |
| 2 | 88.490 | 55.140 | 62.170 | 40.636 |
| 3 | 153.340 | 57.355 | 112.365 | 40.832 |
| 4 | 82.730 | 59.810 | 57.795 | 43.390 |
| 6 | 89.655 | 49.807 | 62.940 | 36.154 |
| 7 | 149.015 | 40.632 | 108.86 | 28.311 |
| 9 | 137.185 | 48.658 | 99.55 | 34.540 |

Note: Coordinates are in millimeters, coordinate system for each photo is parallel to the pixel grid, origin at the lower left corner of the grid.

Next, estimates were made of the camera interior and exterior orientation parameters. The location in space was estimated by offsets in the local coordinate system from control point 4. Image plane orientation was estimated by calculating $\omega$, $\phi$, and $\kappa$ from an assumed camera view direction with the focal axis horizontal. The Principal Point was assumed to be in the center of the image, and the focal length was assumed to be 6 in. (approx. 150 mm.).

The control point image and space coordinates, plus the initial parameter estimates, were used to solve for the actual orientation parameters using a macro program written in a Quattro Pro spreadsheet. The results are shown in Table 3. The details of the Quattro Pro program are given in Appendix C.

Table 3. Resection solutions for orientation parameters

| | $X_C$ | $Y_C$ | $Z_C$ | $\omega$ | $\phi$ | $\kappa$ | f | $x_p$ | $y_p$ |
|---|---|---|---|---|---|---|---|---|---|
| Gifford photo | | | | | | | | | |
| est. | 585.7 | 3964.9 | 52.3 | 90 | -40 | 0 | 150 | 106.07 | 82.33 |
| solved | 592.10 | 3967.30 | 52.27 | 161.88 | -55.21 | 68.45 | 112.09 | 176.75 | 125.21 |
| New photo | | | | | | | | | |
| est. | 585.7 | 3964.9 | 52.3 | 90 | -40 | 0 | 105 | 76.2 | 46.8 |
| solved | 591.30 | 3966.47 | 52.35 | 167.30 | -55.09 | 75.87 | 85.24 | 140.73 | 94.82 |

Note: Space coordinates are meters, angles are decimal degrees, interior orientation parameters are millimeters.

It was hoped that the orientation information could be used to rephotograph the original scene, using a 4x5 view camera, yielding an image that could be compared photogrammetrically to the original. This proved to be impractical, since the camera position turned out to be located in the middle of a highway, still open to automobile traffic, on a blind curve with no shoulders. However, at some risk to life and limb, a quick 35mm snapshot was taken from the approximate camera position (Figure 8). Measurements were taken of the image coordinates of the same control points on a digitized print of the resulting photograph. Table 3 gives the results of the resection solution for the external orientation parameters of this photograph.


Figure 8. New photograph of Shepperd's Dell Bridge

## Applications

The most direct application of a photogrammetric solution of historic photograph location and orientation would be in repeating the original photograph. A modern camera set up with identical orientation parameters will duplicate the original photographic perspective and field of view on the first attempt, at least theoretically, without having to take several photographs, progressively homing in on the orientation at the original point in space. In exchange, the researcher would have to spend time in the field identifying and surveying control points. Whether this would practically take more or less time than traditional methods would depend on the individual situation, but certainly, the progress being made in the precision, accuracy, and speed of GPS surveying instruments will contribute to the practicality of applying this direct method. In addition, the calculations involved, which are dauntingly tedious, can easily be programmed in a personal computer; the matrix operations involved can even be handled by many handheld calculators, a consideration for practical field application.

Once the interior orientation of the original image is known with some precision the historic image can be used to take direct measurements of objects in the field of view. This is accomplished through the obverse solution to the collinearity situation, using the now known elements of exterior and interior orientation to solve for the unknown space coordinates of points whose image coordinates can be measured. The linear form of the two collinearity equations for this situation are:

$$x_a - F_O + v_{x_a} = b_{11}\Delta X_a + b_{12}\Delta Y_a + b_{13}\Delta Z_a \tag{9}$$

$$y_a - G_O + v_{y_a} = b_{21}\Delta X_a + b_{22}\Delta Y_a + b_{23}\Delta Z_a \tag{10}$$

in which the all of the terms involving the known parameters which are held fixed drop out since their respective $\Delta$ terms become zero. The new unknown terms are the *X, Y,* and *Z* space coordinates of the object in question. In these equations, *b* has been used as shorthand for the partial derivatives of the original equations with respect to the new unknowns in order to avoid confusion with the *d* coefficients of equations (4) and (5). Since the two image coordinates of a point contribute two equations, a solution for all three unknown space coordinates is not possible from one photo image. The two equations solve for the collinearity line in space that satisfies the equations; the object position of the point could lie anywhere on the line. Without some other information, such as some scale dimensions in different points of the depth of field of the image, where the object lies on the collinearity line cannot be resolved.

The situation is completely soluble, however, if another overlapping image of the same object is available. In this case two more equations can be developed from the collinearity situation of the second image. In this way any point in the field of view of both photographs can be resolved in all three dimensions of object space. There are many situations where more than one contemporary image exists with the required overlapping fields of view. In such cases, a three dimensional model of the overlapping area can be constructed and measurements taken anywhere in that space.

Images that would provide such coverage could be very valuable to researchers in many fields who are concerned with changes in the landscape over time. Several studies surveyed demonstrated possible applications. McDonald's survey (1995) of mass changes to Collier Glacier, Oregon, over nearly one hundred years utilized both aerial and terrestrial historic photographs. This study might have benefitted from accurate measurements of the terrestrial images used. In these images there may have been sufficient fixed control points to provide fairly accurate space coordinates for changing glacial dimensions even though the coverage was limited to a single photograph. Graf's study (1979) of the changing morphology and dynamics of a stream channel in a mining environment also used historic photographs, but mainly as a subjective guide to mapping vegetation patterns. It is possible that the photographs could also have been applied to accurate stream channel shape measurements had the orientation geometry of the photos been calculated.

The utility of applying non-metric camera images to accurate stream channel measurement was demonstrated by Welch and Jordan (1983), using a 35mm camera and enlarged and digitized images, which yielded results comparable in accuracy to measurements developed on images from metric cameras measured on a conventional photogrammetric comparator. The improvements in digital technology since this study have made these photogrammetric techniques even more available to researchers without access to technical photogrammetric equipment and software.

Many research applications can benefit from extracting precise landscape measurements from the wealth of detail preserved in historic photographs. Inventories of vegetation, with measurements of spatial extent, tree bole sizes, and species distribution, can increase confidence levels of statistical analyses. Geomorphologists can quantify mass movements, creep, landslides, erosion, and other landscape changes in the temporal dimension, at least as far back in time as photography records. For reconstruction studies, archeologists can measure structures and artifacts that have either been displaced or no longer exist. All these applications can benefit from very precise positioning in cases where two or more overlapping photographs are available. Even with one photograph, however, precise orientation in space of the collinearity line upon which an object lies can still allow fairly precise positioning of that object if other existing geometric elements, such as the ground surface, which may be modeled from the existing landscape, can be used as another constraint upon the object's position.

## Suggestions for Further Research

To facilitate the practical application of photogrammetric measurement techniques to historical photographs it would be useful to develop a resection solution program that could run on a personal computer. Such a program would run in a common environment such as Microsoft Windows, without needing any other software, and would provide a simple interface in which to input control point and parameter data, and would output the parameter solutions in a tabular and/or graphic display. In addition, the same program could be used to solve by space intersection the space coordinates of unknown points from the their measured image coordinates in two or more photos with solved orientations.

In order to be practically applied by researchers, a simple method of rapidly measuring the spatial coordinates of control points needs to be developed. It is assumed that this will be facilitated in the near future by the increasing availability of carrier-phase GPS receivers that can provide rapid solutions of sub-centimeter accuracy in near real time. Total station measurements will still be necessary to locate points not easily occupied.

The accuracy of image coordinate measurements made on digitized images depends on the accuracy of the equipment used to digitize from the original medium. It would be useful to analyze the accuracy and consistency attainable by commonly available flat bed scanners. This could be done by scanning a calibrated reseau grid or an image on a stable medium with control point coordinates known from measurements in a conventional calibrated photogrammetric comparator. The results could be used to develop calibration coefficients that could be used in an affine transformation that could be applied to improve the accuracy of measured image coordinates.

## Conclusion

The principles of photogrammetry, applied to the study of historic photographs, can yield many benefits to researchers interested in studying past landscapes. These techniques are also becoming more practical and accessible to non-specialists with the continuing development of precision digital scanners, which can render historic photographs into a medium in which they can easily be measured with high precision. The voluminous calculations necessary in the application of analytic photogrammetry, so long an impediment even in the profession of photogrammetry, can now practically be applied by anyone with a personal computer. The practice of repeat photography can be facilitated by directly calculating the original image's spatial orientation. Precise knowledge of this original orientation can enhance the value of historical images much beyond their recognized importance as subjective snap shots of long past landscapes.

REFERENCES


Abdel-Aziz, Y.I. and H.M. Karara. 1971. Direct Linear Transformation from Comparator Coordinates into Object Space Coordinates in Close-Range Photogrammetry. Papers from the 1971 ASP Symposium on Close-Range Photogrammetry. Falls Church, VA: American Society of Photogrammetry.

Abdel-Aziz, Y.I. and H.M. Karara. 1974. Photogrammetric Potentials of Non-Metric Cameras. Urbana, IL: University of Illinois at Urbana-Champaign.

Atkinson, K.B., Ed. 1980. Developments in Close Range Photogrammetry - 1. London: Applied Science Publishers.

Bopp, Hanspeter and Herbert Krauss. 1978. An Orientation and Calibration Method for Non-Topographic Applications. Photogrammetric Engineering and Remote Sensing 44: 1191-96.

Borchers, Perry E. 1977. Photographic Recording of Cultural Resources. Washington, DC: U.S. Department of the Interior.

Burnside, C.D. 1985. Mapping from Aerial Photographs. New York: John Wiley & Sons.

Dewitt, Bon A. 1996. Initial Approximations for the Three-Dimensional Conformal Coordinate Transformation. Photogrammetric Engineering and Remote Sensing 62: 79-83.

Faig, Wolfgang.1976. Photogrammetric Potentials of Non-Metric Cameras. Photogrammetric Engineering and Remote Sensing 42: 47-49.

Faig, Wolfgang.1975. Calibration of Close-Range Photogrammetric Systems: Mathematic Formulation. Photogrammetric Engineering and Remote Sensing 41: 1479-86.

Goin, Peter. 1992. Stopping Time: Rephotographic Survey of Lake Tahoe. Albuquerque: University of New Mexico Press.

Graf, William L. 1979. Mining and Channel Response. Annals of the Association of American Geographers 69: 262-75.

Gullberg, Jan. 1997. Mathematics: From the Birth of Numbers. New York: W. W. Norton & Co.

Harrison, A.E. 1974. Reoccupying Unmarked Camera Stations for Geological Observations. Geology 2: 469-71.

Hart, Richard H. and William A. Laycock. 1996. Repeat photography on range and forest lands in the western United States. Journal of Range Management 49: 60-67.

Hastings, James Rodney and Raymond M. Turner. 1965. The Changing Mile: An Ecological Study of Vegetation Change With Time in the Lower Mile of an Arid and Semiarid Region. Tucson: University of Arizona Press.

Hattersley-Smith, G. 1966. Symposium on Glacier Mapping. Canadian Journal of Earth Sciences 3: 737-41.

Karara, H.M. and Y.I. Abdel-Aziz. 1974. Accuracy Aspects of Non-Metric Imageries. Photogrammetric Engineering 40: 1107-17.

Karara, H.M. 1972. Simple Cameras for Close-Range Applications. Photogrammetric Engineering 38: 447-51.

Karara, H.M., Ed. 1979. Handbook of Non-Topographic Photogrammetry. Falls Church, VA: American Society of Photogrammetry.

Klett, Mark, Ellen Manchester, and JoAnn Verburg. 1984. Second View: The Rephotographic Survey Project. Albuquerque: University of New Mexico Press.

Malde, Harold E. 1973. Geologic Bench Marks by Terrestrial Photography. Journal of Research U.S. Geological Survey 1: 193-206.

McDonald, Gregory D. 1995. Changes in mass of Collier Glacier, Oregon, 1910-1994. M.S. Thesis, Department of Geosciences, Oregon State University.

Meagher, Mary, and Douglas B. Houston. 1998. Yellowstone and the Biology of Time: Photographs Across a Century. Norman, OK: University of Oklahoma Press.

Moffitt, Francis H. 1970. Photogrammetry. Scranton, PA: International Textbook Co.

Rogers, Garry F., Harold E. Malde, and Raymond M. Turner. 1984. Bibliography of Repeat Photography for Evaluating Landscape Change. Salt Lake City: University of Utah Press.

Rogers, Garry F. 1982. Then and Now: A Photographic History of Vegetation Change in the Central Great Basin Desert. Salt Lake City: University of Utah Press.

Sallach, Barbara Kay. 1986. Vegetation Changes in New Mexico Documented by Repeat Photography. M.S. Thesis, Department of Biology, New Mexico State University.

Skovlin, Jon M., and Jack Ward Thomas. 1995. Interpreting Long-Term Trends in Blue Mountain Ecosystems from Repeat Photography. Research Paper PNW-GTR-315. Portland, OR: U. S. Department of Agriculture, Forest Service, Pacific Northwest Research Station.

Stephens, Hal G., and Eugene M. Shoemaker. 1987. In the Footsteps of John Wesley Powell: An Album of Comparative Photographs of the Green and Colorado Rivers, 1871-72 and 1968. Boulder, CO: Johnson Books.

Thompson, Morris M, Ed. 1966. Manual of Photogrammetry, Third Edition. Falls Church, VA: American Society of Photogrammetry.

United States Dept. of Agriculture. 1993. Snapshot in Time: Repeat Photography on the Boise National Forest 1870-1992. U. S. Department of Agriculture, Boise National Forest, Intermountain Region.

Webb, Robert H. 1996. Grand Canyon: A Century of Change. Tucson: University of Arizona Press.

Welch, R., and T. R. Jordan. 1983. Analytical Non-Metric Close-Range Photogrammetry for Monitoring Stream Channel Erosion. Photogrammetric Engineering and Remote Sensing 49: 367-74.

Wolf, Paul R., and Bon A. Dewitt. 2000. Elements of Photogrammetry: With Applications in GIS. Boston: McGraw Hill.

# APPENDIX A

## DERIVATION OF THE COLLINEARITY EQUATIONS

The ultimate goal is to express the coordinates of the image point, $x_a$ and $y_a$ in Fig. 4, in an arbitrary orthogonal coordinate measurement system in the image plane, in terms of the space system coordinates, $X_A$, $Y_A$, and $Z_A$, of the object. In this derivation the measurements are related to the positive image plane, analogous to the original negative plane on the other side of the focal node, but geometrically more straightforward. Note that it is important to relate all measurements in the image plane to the Principal Point, PP, which is where a line perpendicular to the image plane and passing through the focal node of the lens, C, intersects the image plane. The arbitrary coordinate system used is related to the coordinate system parallel to the arbitrary system but centered on the Principal Point by the translation offsets $x_o$, $y_o$, which are the arbitrary system coordinates of the Principal Point.

The first step is to transform the image point *a* coordinates from the coordinate system based on the image plane to an intermediate system with the same origin, the camera position in space, but with axes parallel to the object space system (Fig. A1). This is accomplished by rotating the camera system axes around the intermediate axes, $x',y',z'$, in order, by the angles $\omega$, $\phi$, $\kappa$ until the original axes are parallel to the spatial system coordinate axes. This is accomplished mathematically by the transformation equations below, the derivation of which is detailed in Wolf (535-39), Thompson (46-48), or Soffit (89-92):

$$x_a - x_o = m_{11}x'_a + m_{12}y'_a + m_{13}z'_a \tag{A-1}$$

$$y_a - y_o = m_{21}x'_a + m_{22}y'_a + m_{23}z'_a \tag{A-2}$$

$$z = m_{31}x'_a + m_{32}y'_a + m_{33}z'_a \tag{A-3}$$

Note that $z$ is equal to $-f$, the focal length of the measured image. The $m$ coefficients are shorthand for the transformation matrix coefficients, listed below:

$$\begin{aligned}
m_{11} &= \cos\phi\cos\kappa \\
m_{12} &= \sin\omega\sin\phi\cos\kappa + \cos\omega\sin\kappa \\
m_{13} &= -\cos\omega\sin\phi\cos\kappa + \sin\omega\sin\kappa \\
m_{21} &= -\cos\phi\sin\kappa \\
m_{22} &= -\sin\omega\sin\phi\sin\kappa + \cos\omega\cos\kappa \\
m_{23} &= \cos\omega\sin\phi\sin\kappa + \sin\omega\cos\kappa \\
m_{31} &= \sin\phi \\
m_{32} &= -\sin\omega\cos\phi \\
m_{33} &= \cos\omega\cos\phi
\end{aligned}$$

From Fig. A1 we see that the line connecting the camera station C, the image point *a*, and the object point A forms the common side of similar triangles so that:

$$\frac{x'_a}{X_A - X_C} = \frac{y'_a}{Y_A - Y_C} = \frac{z'_a}{Z_A - Z_C} \tag{A-4}$$

Expressing the coordinates in terms of $z$' results in:

$$x'_a = \left( \frac{X_A - X_C}{Z_A - Z_C} \right) z'_a \tag{A-5}$$

$$y'_a = \left( \frac{Y_A - Y_C}{Z_A - Z_C} \right) z'_a \tag{A-6}$$

$$z'_a = \left( \frac{Z_A - Z_C}{Z_A - Z_C} \right) z'_a \tag{A-7}$$

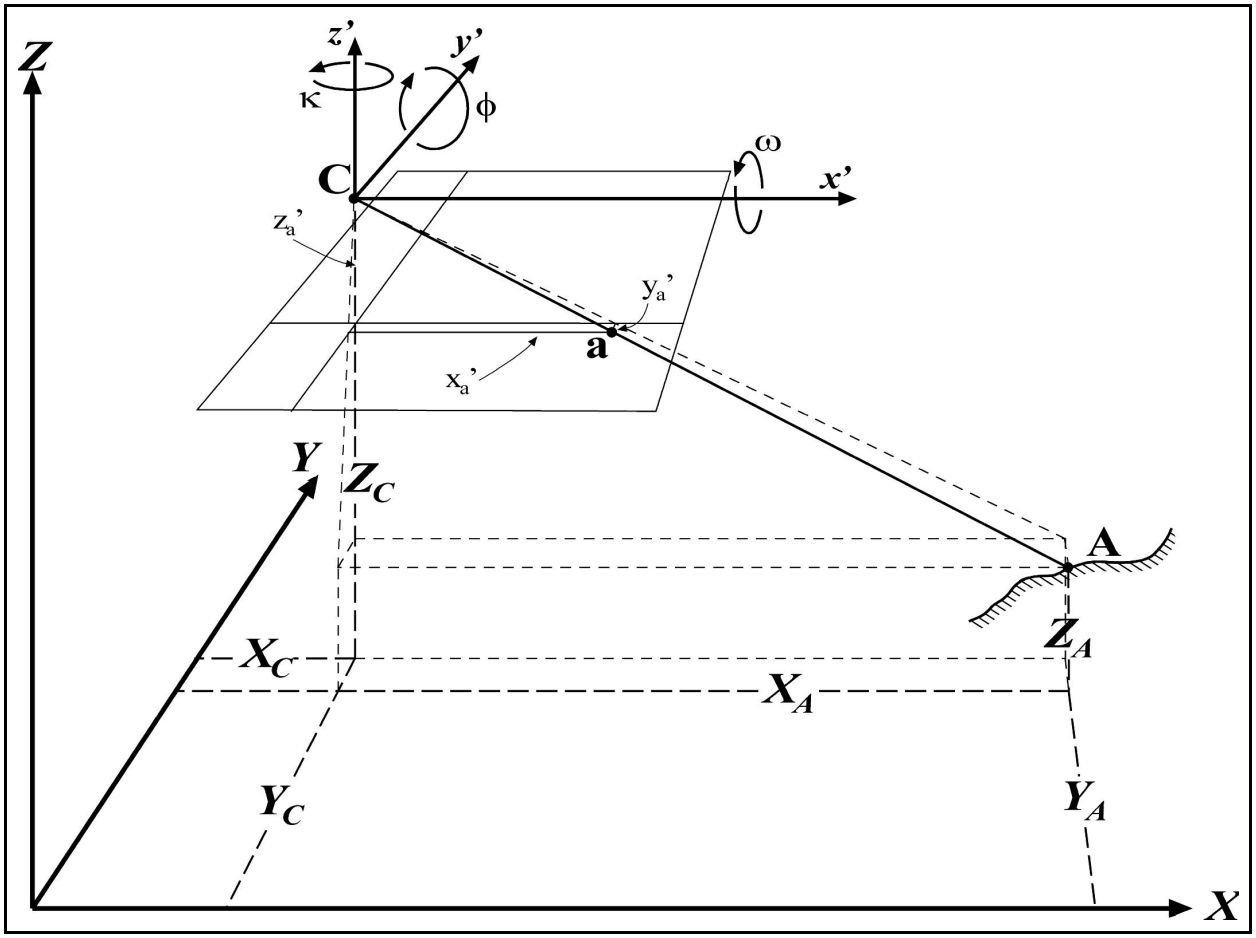


Figure A1. Orthogonal image coordinate system

Substituting into the rotational transformation equations, (A-1)-(A-3):

$$x_a - x_o = m_{11}\left(\frac{X_A - X_C}{Z_A - Z_C}\right)z'_a + m_{12}\left(\frac{Y_A - Y_C}{Z_A - Z_C}\right)z'_a + m_{13}\left(\frac{Z_A - Z_C}{Z_A - Z_C}\right)z'_a \qquad \text{(A-8)}$$

$$y_a - y_o = m_{21}\left(\frac{X_A - X_C}{Z_A - Z_C}\right)z'_a + m_{22}\left(\frac{Y_A - Y_C}{Z_A - Z_C}\right)z'_a + m_{23}\left(\frac{Z_A - Z_C}{Z_A - Z_C}\right)z'_a \qquad \text{(A-9)}$$

$$z = m_{31}\left(\frac{X_A - X_C}{Z_A - Z_C}\right)z'_a + m_{32}\left(\frac{Y_A - Y_C}{Z_A - Z_C}\right)z'_a + m_{33}\left(\frac{Z_A - Z_C}{Z_A - Z_C}\right)z'_a \qquad \text{(A-10)}$$

Dividing (A-8) and (A-9) by (A-10), and cancelling the common term $z'_a/(Z_A - Z_C)$ on the right sides:

$$\frac{x_a - x_o}{z} = \frac{m_{11}(X_A - X_C) + m_{12}(Y_A - Y_C) + m_{13}(Z_A - Z_C)}{m_{31}(X_A - X_C) + m_{32}(Y_A - Y_C) + m_{33}(Z_A - Z_C)} \tag{A-11}$$

$$\frac{y_a - y_o}{z} = \frac{m_{21}(X_A - X_C) + m_{22}(Y_A - Y_C) + m_{23}(Z_A - Z_C)}{m_{31}(X_A - X_C) + m_{32}(Y_A - Y_C) + m_{33}(Z_A - Z_C)} \tag{A-12}$$

more commonly expressed as below, recognizing that $z = -f$:

$$x_a = x_o - f\left[\frac{m_{11}(X_A - X_C) + m_{12}(Y_A - Y_C) + m_{13}(Z_A - Z_C)}{m_{31}(X_A - X_C) + m_{32}(Y_A - Y_C) + m_{33}(Z_A - Z_C)}\right] \tag{A-13}$$

$$y_a = y_o - f\left[\frac{m_{21}(X_A - X_C) + m_{22}(Y_A - Y_C) + m_{23}(Z_A - Z_C)}{m_{31}(X_A - X_C) + m_{32}(Y_A - Y_C) + m_{33}(Z_A - Z_C)}\right] \tag{A-14}$$

APPENDIX B

LINEARIZING THE COLLINEARITY EQUATIONS

Since the collinearity equations are non-linear functions with respect to most of the variables, it is necessary to linearize them so that they can be simultaneously solved for the several unknowns. In addition, in their linear form they can be developed into a set of normal equations enabling a least squares solution.

The Taylor power series expansion can be used to expand a continuous monotonic function of the general form, for a function of a variable $x$, $f(x)$:

$$f(x) = \sum_{k=0}^{\infty} \frac{f^{(k)}(c)}{k!}(x-c)^k \tag{B-1}$$

where $c$ is the point around which the series is centered and $f^{(k)}$ denotes the $k$th derivative of $f(x)$, evaluated at $c$. It would be rather tedious to evaluate this series out to infinity. Fortunately, as can be seen, for values of $x$ very close to $c$, all but the first couple of terms become insignificant. Therefore a very good approximation can be made using only the first two terms:

$$f(x) \approx f(c) + f'(c)(x-c) \tag{B-2}$$

For a function of more than one variable, the same approximation applies, with the first derivative term being replaced by terms representing the partial derivative of $f(x)$ with respect to each variable:

$$\begin{aligned} f(a,b,c,\ldots) = {} & f(a_o,b_o,c_o,\ldots) + \frac{\partial f}{\partial a}(a-a_o) \\ & + \frac{\partial f}{\partial b}(b-b_o) + \frac{\partial f}{\partial c}(c-c_o) + \ldots \end{aligned} \tag{B-3}$$

where $a_o$, etc. represent the convergent, or initial, estimated values, the partial derivatives being evaluated at those values (Burnside 331; Gullberg 767).

The two collinearity equations, (A-13) and (A-14), can be similarly expanded, using $F$ to denote the expression for $x_a$ and $G$ for $y_a$, with terms for the 9 unknowns of the interior and exterior orientation:

$$F = x_a = F_O + \left(\frac{\partial F}{\partial \omega}\right)_o (\omega - \omega_o) + \left(\frac{\partial F}{\partial \phi}\right)_o (\phi - \phi_o) + \left(\frac{\partial F}{\partial \kappa}\right)_o (\kappa - \kappa_o)$$
$$+ \left(\frac{\partial F}{\partial X_C}\right)_o (X_C - X_{C_o}) + \left(\frac{\partial F}{\partial Y_C}\right)_o (Y_C - Y_{C_o}) + \left(\frac{\partial F}{\partial Z_C}\right)_o (Z_C - Z_{C_o}) \qquad \text{(B-4)}$$
$$+ \left(\frac{\partial F}{\partial x_o}\right)_o (x_o - x_{o_o}) + \left(\frac{\partial F}{\partial y_o}\right)_o (y_o - y_{o_o}) + \left(\frac{\partial F}{\partial f}\right)_o (f - f_o)$$

$$G = y_a = G_O + \left(\frac{\partial G}{\partial \omega}\right)_o (\omega - \omega_o) + \left(\frac{\partial G}{\partial \phi}\right)_o (\phi - \phi_o) + \left(\frac{\partial G}{\partial \kappa}\right)_o (\kappa - \kappa_o)$$
$$+ \left(\frac{\partial G}{\partial X_C}\right)_o (X_C - X_{C_o}) + \left(\frac{\partial G}{\partial Y_C}\right)_o (Y_C - Y_{C_o}) + \left(\frac{\partial G}{\partial Z_C}\right)_o (Z_C - Z_{C_o}) \qquad \text{(B-5)}$$
$$+ \left(\frac{\partial G}{\partial x_o}\right)_o (x_o - x_{o_o}) + \left(\frac{\partial G}{\partial y_o}\right)_o (y_o - y_{o_o}) + \left(\frac{\partial G}{\partial f}\right)_o (f - f_o)$$

Here each of the partial derivatives is evaluated using the convergent or initial values of the variables and each of the terms of the form $(\omega - \omega_o)$ can be considered the corrections to be applied to the initial values, and are the unknowns that are solved for. $F_O$ and $G_O$ represent the full respective functions evaluated using all of the initial values, both fixed and estimated. Note that only unknown variables of the functions appear in the partial differential terms, since any known values are held fixed, and so their correction factors become zero. These linear equations can more simply be expressed, including a variance factor to allow for a least squares solution, as:

$$x_a - F_O + v_{x_a} = d_{11}\Delta\omega + d_{12}\Delta\phi + d_{13}\Delta\kappa + d_{14}\Delta X_C + d_{15}\Delta Y_C + d_{16}\Delta Z_C + d_{17}\Delta x_o + d_{18}\Delta y_o + d_{19}\Delta f \qquad \text{(B-6)}$$

$$y_a - G_O + v_{y_a} = d_{21}\Delta\omega + d_{22}\Delta\phi + d_{23}\Delta\kappa + d_{24}\Delta X_C + d_{25}\Delta Y_C + d_{26}\Delta Z_C + d_{27}\Delta x_o + d_{28}\Delta y_o + d_{29}\Delta f \qquad \text{(B-7)}$$

where we use the *d*'s as shorthand for the derivative expressions in (B-4) and (B-5) and the Δ's to represent the differences to be solved for.

It will be convenient in evaluating the partial derivatives to use the following expressions in representing the collinearity equations:

Let
$$r = m_{11}(X_A - X_C) + m_{12}(Y_A - Y_C) + m_{13}(Z_A - Z_C)$$
$$s = m_{21}(X_A - X_C) + m_{22}(Y_A - Y_C) + m_{23}(Z_A - Z_C)$$
$$q = m_{31}(X_A - X_C) + m_{32}(Y_A - Y_C) + m_{33}(Z_A - Z_C)$$

So that the collinearity equations become:

$$F = x_a = x_o - f\frac{r}{q} \tag{B-7}$$

$$G = y_a = y_o - f\frac{s}{q} \tag{B-8}$$

In order to solve the equations we need to evaluate the *d* terms, which are the partial derivatives of the collinearity equations with respect to the unknown variables in question. As an example, we will evaluate the $d_{11}$ term, which relates to the unknown ω.

$$d_{11} = \frac{\partial F}{\partial \omega} = 0 - f\left[\frac{\frac{\partial r}{\partial \omega}q - r\frac{\partial q}{\partial \omega}}{q^2}\right]$$

by the derivative of quotient functions, *r* and *q* being the only functions that contain ω, but

$$\begin{aligned} r &= m_{11}(X_A - X_C) + m_{12}(Y_A - Y_C) + m_{13}(Z_A - Z_C) \\ &= \cos\phi\cos\kappa(X_A - X_C) + (\sin\omega\sin\phi\cos\kappa + \cos\omega\sin\kappa)(Y_A - Y_C) \\ &\quad + (-\cos\omega\sin\phi\cos\kappa + \sin\omega\sin\kappa)(Z_A - Z_C) \end{aligned}$$

$$\begin{aligned} \therefore \quad \frac{\partial r}{\partial \omega} &= 0 + (\cos\omega\sin\phi\cos - \sin\omega\sin\kappa)(Y_A - Y_C) \\ &\quad + (\sin\omega\sin\phi\cos\kappa + \cos\omega\sin\kappa)(Z_A - Z_C) \\ &= -m_{13}(Y_A - Y_C) + m_{12}(Z_A - Z_C) \end{aligned}$$

similarly we can find that

$$\frac{\partial q}{\partial \omega} = -m_{33}(Y_A - Y_C) + m_{32}(Z_A - Z_C)$$

substituting and simplifying

$$d_{11} =$$

$$0 - f\left[\frac{q\left[-m_{13}(Y_A - Y_C) + m_{12}(Z_A - Z_C)\right] - r\left[-m_{33}(Y_A - Y_C) + m_{32}(Z_A - Z_C)\right]}{q^2}\right]$$

$$= \frac{f}{q^2}\left[r\left[-m_{33}(Y_A - Y_C) + m_{32}(Z_A - Z_C)\right] - q\left[-m_{13}(Y_A - Y_C) + m_{12}(Z_A - Z_C)\right]\right]$$

The remaining partial derivatives are similarly developed. The following is a list of all the necessary coefficients for the equations solving for the nine unknowns, using the shorthand *m* elements where possible:

$$d_{11} = \frac{f}{q^2}\left[r\left[-m_{33}(Y_A - Y_C) + m_{32}(Z_A - Z_C)\right] - q\left[-m_{13}(Y_A - Y_C) + m_{12}(Z_A - Z_C)\right]\right]$$

$$d_{12} = \frac{f}{q^2}[r[\cos\phi(X_A - X_C) + \sin\omega\sin\phi(Y_A - Y_C) - \cos\omega\sin\phi(Z_A - Z_C)]$$
$$- q[-\sin\phi\cos\kappa(X_A - X_C) + \sin\omega\cos\phi\cos\kappa(Y_A - Y_C)$$
$$- \cos\omega\cos\phi\cos\kappa(Z_A - Z_C)]]$$

$$d_{13} = -\frac{f}{q}[m_{21}(X_A - X_C) + m_{22}(Y_A - Y_C) + m_{23}(Z_A - Z_C)]$$

$$d_{14} = -\frac{f}{q^2}(rm_{31} - qm_{11})$$

$$d_{15} = -\frac{f}{q^2}(rm_{32} - qm_{12})$$

$$d_{16} = -\frac{f}{q^2}(rm_{33} - qm_{13})$$

$$d_{17} = 1$$

$$d_{18} = 0$$

$$d_{19} = -\frac{r}{q}$$

$$d_{21} = \frac{f}{q^2}\left[s\left[-m_{33}(Y_A - Y_C) + m_{32}(Z_A - Z_C)\right] - q\left[-m_{23}(Y_A - Y_C) + m_{22}(Z_A - Z_C)\right]\right]$$

$$d_{22} = \frac{f}{q^2}[s[\cos\phi(X_A - X_C) + \sin\omega\sin\phi(Y_A - Y_C) - \cos\omega\sin\phi(Z_A - Z_C)]$$
$$- q[\sin\phi\sin\kappa(X_A - X_C) + \sin\omega\cos\phi\sin\kappa(Y_A - Y_C)$$
$$+ \cos\omega\cos\phi\sin\kappa(Z_A - Z_C)]]$$

$$d_{23} = \frac{f}{q}[m_{11}(X_A - X_C) + m_{12}(Y_A - Y_C) + m_{13}(Z_A - Z_C)]$$

$$d_{24} = -\frac{f}{q^2}(sm_{31} - qm_{21})$$

$$d_{25} = -\frac{f}{q^2}(sm_{32} - qm_{22})$$

$$d_{26} = -\frac{f}{q^2}(sm_{33} - qm_{23})$$

$$d_{27} = 0$$

$$d_{28} = 1$$

$$d_{29} = -\frac{s}{q}$$

# APPENDIX C

## QUATTRO PRO RESECTION PROGRAM

### Initial Condition Sheet

| | | | | | | |
|---|---|---|---|---|---|---|
| Collinearity Resection Solution | | | | | | |
| | Zan Strausz, 30 March 2001 | | | | | |
| | Solving for interior and exterior orientation (9 unknowns) | | | | | |
| | | | | | | |
| INITIAL CONDITIONS | | | | | | |
| | | | | | | |
| measured coordinates | | | | | | |
| | | Photo | | | Ground | |
| | Cont. Pts | xp | yp | X | Y | Z |
| | A | 109.745 | 54.550 | 639.16 | 4005.30 | 52.78 |
| | B | 88.490 | 55.140 | 631.70 | 4008.36 | 52.79 |
| | C | 153.340 | 57.355 | 608.17 | 3973.78 | 52.79 |
| | D | 82.730 | 59.810 | 600.74 | 3976.90 | 52.72 |
| | E | 89.655 | 49.807 | 633.38 | 4008.09 | 51.32 |
| | F | 149.015 | 40.632 | 608.14 | 3974.27 | 50.98 |
| | G | 137.185 | 48.658 | 612.52 | 3978.38 | 51.68 |
| | H | | | | | |
| | I | | | | | |
| | J | | | | | |
| | K | | | | | |
| | L | | | | | |
| | nocp | 7 | | | | |
| | | | | | | |
| | | | | | | |
| initial estimates | | | | iofixed? | no | |
| | omega | 90 | | | | |
| | phi | -45 | | nounk | 9 | |
| | kappa | 0 | | | | |
| | XC0 | 585.7 | | | | |
| | YC0 | 3964.9 | | | | |
| | ZC0 | 52.3 | | | | |
| | f | 80 | | | | |
| | x_0 | 180 | | | | |
| | y_0 | 120 | | | | |
| | | | | | | |
| maximum diffs | | | | | | |
| | dangle | 0.0001 | | | | |
| | dcoord | 0.01 | | | | |
| | | | | | | |
| maximum iterations | | | | | | |
| | imax | 50 | | | | |

Iteration Sheet

| | | | | | | | | | |
|---|---|---|---|---|---|---|---|---|---|
| ITERATIONS | | | | | | | | | |
| | it_no | 28 | | | | | | | |
| initial estimates | | deg. | rad. | | | | | | |
| | omega | 161.876 | 2.82526 | | XC | 592.104 | | foc | 112.088 |
| | phi | -55.205 | -0.9635 | | YC | 3967.3 | | PPx | 176.752 |
| | kappa | 68.4518 | 1.19471 | | ZC | 52.2709 | | PPy | 125.206 |
| | alpha | 77.8025 | | solved diffs. | | rad. | deg. | | |
| | tilt | 122.842 | | | do | 1.3E-06 | 7.3E-05 | | |
| | swing | 0.18334 | | | dp | 4.8E-07 | 2.7E-05 | | |
| | | | | | dk | 9.2E-07 | 5.3E-05 | | |
| | | | | | dXC | 3.2E-06 | | | |
| rotation matrix | | | | | dYC | 3.3E-06 | | | |
| | m_11 | 0.20959 | | | dZC | 2E-07 | | | |
| | m_12 | -0.9778 | | | dx_0 | 1.7E-05 | | | |
| | m_13 | 0.00269 | | | dy_0 | 1.8E-05 | | | |
| | m_21 | -0.5308 | | | df | -0.0001 | | | |
| | m_22 | -0.1115 | | | | | | | |
| | m_23 | 0.84016 | | | | | | | |
| | m_31 | -0.8212 | | max diff test | | | | | |
| | m_32 | -0.1775 | | | maxtst | 1 | | | |
| | m_33 | -0.5423 | | | | | | | |
| D_matrix | -31.574 | 16.5993 | -70.651 | -1.7192 | 2.13966 | -0.8022 | 1 | 0 | -0.5977 |
| | -110.25 | -99.364 | 66.9922 | 0.03225 | -0.0011 | -2.9013 | 0 | 1 | -0.6303 |
| | -50.991 | 15.1757 | -70.34 | -2.4103 | 2.33969 | -1.2123 | 1 | 0 | -0.7945 |
| | -135.53 | -86.873 | 89.0511 | 0.04311 | 0.00016 | -3.3008 | 0 | 1 | -0.6275 |
| | -9.3455 | 30.1158 | -67.544 | -2.8833 | 7.21762 | -0.864 | 1 | 0 | -0.2029 |
| | -57.974 | -120.68 | 22.7436 | 0.27512 | 0.03438 | -8.9435 | 0 | 1 | -0.6026 |
| | -59.038 | 19.0857 | -65.423 | -11.132 | 10.2794 | -5.6688 | 1 | 0 | -0.838 |
| | -137.73 | -80.326 | 93.9346 | 0.63778 | 0.09727 | -14.343 | 0 | 1 | -0.5837 |
| | -45.033 | 11.727 | -75.2 | -2.3208 | 2.3214 | -1.1581 | 1 | 0 | -0.769 |
| | -135.54 | -92.774 | 86.1903 | -0.0557 | -0.0211 | -3.3223 | 0 | 1 | -0.6709 |
| | 1.89701 | 23.8835 | -84.827 | -3.4083 | 7.63002 | -1.1409 | 1 | 0 | -0.2523 |
| | -71.527 | -137.28 | 28.2783 | -0.7419 | -0.1872 | -10.227 | 0 | 1 | -0.7568 |
| | -9.9185 | 21.0487 | -76.506 | -3.0561 | 5.56764 | -1.1921 | 1 | 0 | -0.3561 |
| | -81.675 | -120.54 | 39.9153 | -0.1812 | -0.0591 | -7.3681 | 0 | 1 | -0.6826 |

Blocks containing matrices $\mathbf{L}$, $\mathbf{D}^{\mathbf{T}}$, $\mathbf{D}^{\mathbf{T}}\mathbf{D}$, $\mathbf{D}^{\mathbf{T}}\mathbf{L}$, and $(\mathbf{D}^{\mathbf{T}}\mathbf{D})^{-1}$ are also included on this sheet, but not shown here.

Control Point Calculation Sheet

| CONTROL POINT SOLUTIONS | | | | | | | | | |
|---|---|---|---|---|---|---|---|---|---|
| | | | | | | | | | |
| Control points | cp_no | 7 | | | | | | | |
| | | | | | | | | | |
| Ground Coord. Diffs | | | Current Pt | | | | | | |
| | DX | 20.4162 | | xp | yp | X | Y | Z | |
| | DY | 11.0802 | | 137.185 | 48.658 | 612.52 | 3978.38 | 51.68 | |
| | DZ | -0.5909 | | | | | | | |
| | | | | | | | | | |
| | | | | | | | | | |
| | | | | | | | | | |
| | | | | | | | | | |
| r,s,q | | | | | | | | | |
| | r | -6.5567 | | | | | | | |
| | s | -12.567 | | | | | | | |
| | q | -18.412 | | | | | | | |
| | | | | | | | | | |
| | | | | | | | | | |
| d coefficients | | | P coord diffs. | | | | | | |
| | d_11 | -9.9185 | | xp_F | 0.34808 | | | | |
| | d_12 | 21.0485 | | yp_G | -0.042 | | | | |
| | d_13 | -76.506 | | | | | | | |
| | d_14 | -3.0561 | | | | | | | |
| | d_15 | 5.56763 | | | | | | | |
| | d_16 | -1.1921 | | | | | | | |
| | d_17 | 1 | | | | | | | |
| | d_18 | 0 | | | | | | | |
| | d_19 | -0.3561 | | | | | | | |
| | d_21 | -81.675 | | | | | | | |
| | d_22 | -120.54 | | | | | | | |
| | d_23 | 39.9153 | | | | | | | |
| | d_24 | -0.1812 | | | | | | | |
| | d_25 | -0.0591 | | | | | | | |
| | d_26 | -7.3681 | | | | | | | |
| | d_27 | 0 | | | | | | | |
| | d_28 | 1 | | | | | | | |
| | d_29 | -0.6826 | | | | | | | |

Residual Calculation Sheet

| RESIDUALS | | | | | |
|---|---|---|---|---|---|
| | | | | | |
| v_xa | 0.014984 | DXX | 8.7E-07 | L_res | -0.01498 |
| v_ya | 0.005451 | | -2.2E-05 | | -0.00547 |
| v_xb | -0.78895 | | 4.7E-07 | | 0.78895 |
| v_yb | -0.27371 | | -2.8E-05 | | 0.273687 |
| v_xc | 0.668646 | | -9.9E-07 | | -0.66865 |
| v_yc | 0.306884 | | -1.2E-05 | | -0.3069 |
| v_xd | 0.08764 | | 1.7E-07 | | -0.08764 |
| v_yd | -0.02732 | | -2.9E-05 | | 0.027294 |
| v_xe | 0.906888 | | -1.1E-06 | | -0.90689 |
| v_ye | 0.19949 | | -2.8E-05 | | -0.19952 |
| v_xf | -0.54113 | | 5.5E-07 | | 0.54113 |
| v_yf | -0.25281 | | -1.5E-05 | | 0.252798 |
| v_xg | -0.34808 | | 9.4E-09 | | 0.348079 |
| v_yg | 0.042025 | | -1.6E-05 | | -0.04204 |
| v_xh | 0 | | | | |
| v_yh | 0 | | | | |
| v_xi | 0 | | | | |
| v_yi | 0 | | | | |
| v_xj | 0 | | | | |
| v_yj | 0 | | | | |
| v_xk | 0 | | | | |
| v_yk | 0 | | | | |
| v_xl | 0 | | | | |
| v_yl | 0 | | | | |

# List of Cell Formulae

| Cell | Address | Formula |
|---|---|---|
| nocp | initial:B22 | @COUNT(C10..C21) |
| orad | iteration:D7 | @RADIANS(omega) |
| prad | iteration:D8 | @RADIANS(phi) |
| krad | iteration:D9 | @RADIANS(kappa) |
| | iteration:C11 | @DEGREES(@ATAN((-m_31)/(-m_32))) |
| | iteration:C12 | @DEGREES(@ACOS(m_33)) |
| | iteration:C13 | @DEGREES(@ATAN((-m_13)/(-m_23))) |
| dodeg | iteration:H12 | @DEGREES(do) |
| dpdeg | iteration:H13 | @DEGREES(dp) |
| dkdeg | iteration:H14 | @DEGREES(dk) |
| maxtest | iteration:G24 | @AND(@ABS(dodeg)<dangle,@ABS(dpdeg)<dangle,@ABS(dkdeg)<dangle,@ABS(dXC)<dcoord,@ABS(dYC)<dcoord,@ABS(dZC)<dcoord,@ABS(dx_0)<dcoord,@ABS(dy_0)<dcoord,@ABS(df)<dcoord) |
| m_11 | iteration:C17 | @COS(prad)*@COS(krad) |
| m_12 | iteration:C18 | @SIN(orad)*@SIN(prad)*@COS(krad)+@COS(orad)*@SIN(krad) |
| M_13 | iteration:C19 | -(@COS(orad)*@SIN(prad)*@COS(krad))+@SIN(orad)*@SIN(krad) |
| m_21 | iteration:C20 | -@COS(prad)*@SIN(krad) |
| m_22 | iteration:C21 | -(@SIN(orad)*@SIN(prad)*@SIN(krad))+@COS(orad)*@COS(krad) |
| m_23 | iteration:C22 | @COS(orad)*@SIN(prad)*@SIN(krad)+@SIN(orad)*@COS(krad) |
| m_31 | iteration:C23 | @SIN(prad) |
| m_32 | iteration:C24 | -@SIN(orad)*@COS(prad) |
| m_33 | iteration:C25 | @COS(orad)*@COS(prad) |
| DX | ContPt:C7 | +X-XC |
| DY | ContPt:C8 | +Y-YC |
| DZ | ContPt:C9 | +Z-ZC |
| r | ContPt:C15 | +m_11*DX+m_12*DY+m_13*DZ |
| s | ContPt:C16 | +m_21*DX+m_22*DY+m_23*DZ |
| q | ContPt:C17 | +m_31*DX+m_32*DY+m_33*DZ |
| d_11 | ContPt:C21 | (foc/(q^2))*(r*(-m_33*DY+m_32*DZ)-q*(-m_13*DY+m_12*DZ)) |
| d_12 | ContPt:C22 | (foc/(q^2))*(r*(@COS(prad)*DX+@SIN(orad)*@SIN(prad)*DY-@COS(orad)*@SIN(prad)*DZ)-q*(-@SIN(prad)*@COS(krad)*DX+@SIN(orad)*@COS(prad)*@COS(krad)*DY-@COS(orad)*@COS(prad)*@COS(krad)*DZ)) |
| d_13 | ContPt:C23 | -(foc/q)*(m_21*DX+m_22*DY+m_23*DZ) |
| d_14 | ContPt:C24 | -(foc/q^2)*(r*m_31-q*m_11) |
| d_15 | ContPt:C25 | -(foc/q^2)*(r*m_32-q*m_12) |
| d_16 | ContPt:C26 | -(foc/q^2)*(r*m_33-q*m_13) |
| d_17 | ContPt:C27 | 1 |
| d_18 | ContPt:C28 | 0 |
| d_19 | ContPt:C29 | -r/q |
| d_21 | ContPt:C30 | (foc/q^2)*(s*(-m_33*DY+m_32*DZ)-q*(-m_23*DY+m_22*DZ)) |
| d_22 | ContPt:C31 | (foc/q^2)*(s*(@COS(prad)*DX+@SIN(orad)*@SIN(prad)*DY-@COS(orad)*@SIN(prad)*DZ)-q*(@SIN(prad)*@SIN(krad)*DX+@SIN(orad)*@COS(prad)*@SIN(krad)*DY+@COS(orad)*@COS(prad)*@SIN(krad)*DZ)) |
| d_23 | ContPt:C32 | (foc/q)*(m_11*DX+m_12*DY+m_13*DZ) |
| d_24 | ContPt:C33 | -(foc/q^2)*(s*m_31-q*m_21) |
| d_25 | ContPt:C34 | -(foc/q^2)*(s*m_32-q*m_22) |
| d_26 | ContPt:C35 | -(foc/q^2)*(s*m_33-q*m_23) |
| d_27 | ContPt:C36 | 0 |
| d_28 | ContPt:C37 | 1 |
| d_29 | ContPt:C38 | -s/q |
| xp_F | ContPt:G21 | +xp-PPx+(foc*r/q) |
| yp_G | ContPt:G22 | +yp-PPy+(foc*s/q) |
| | Residuals:B3 | +DXX-L_res |
| | Residuals:B4 | +E4-G4 |
| | Residuals:B5 | +E5-G5 |
| | Residuals:B6 | +E6-G6 |
| | Residuals:B7 | +E7-G7 |
| | Residuals:B8 | +E8-G8 |
| | Residuals:B9 | +E9-G9 |
| | Residuals:B10 | +E10-G10 |
| | Residuals:B11 | +E11-G11 |
| | Residuals:B12 | +E12-G12 |

| Cell | Address | Formula |
|---|---|---|
| | Residuals:B13 | +E13-G13 |
| | Residuals:B14 | +E14-G14 |
| | Residuals:B15 | +E15-G15 |
| | Residuals:B16 | +E16-G16 |
| | Residuals:B17 | +E17-G17 |
| | Residuals:B18 | +E18-G18 |
| | Residuals:B19 | +E19-G19 |
| | Residuals:B20 | +E20-G20 |
| | Residuals:B21 | +E21-G21 |
| | Residuals:B22 | +E22-G22 |
| | Residuals:B23 | +E23-G23 |
| | Residuals:B24 | +E24-G24 |
| | Residuals:B25 | +E25-G25 |
| | Residuals:B26 | +E26-G26 |

# Macro Commands

| Name | Code |
|---|---|
| | |
| _initialize | {;set initial parameters} |
| | {;set counters to 0} |
| | {let it_no,0} |
| | {;no of unknowns, control pts} |
| | {IF iofixed?="yes"}{let nounk,6} |
| | {IF iofixed?<>"yes"}{let nounk,9} |
| | {;size and name matrix blocks} |
| | {_sizmat} |
| | {;clear diffs} |
| | {blank diffs} |
| | {;put starting estimates in iteration} |
| | {let omega,omega0} |
| | {let phi,phi0} |
| | {let kappa,kappa0} |
| | {let XC,XC0} |
| | {let YC,YC0} |
| | {let ZC,ZC0} |
| | {let foc,f_0} |
| | {let PPx,x_0} |
| | {let PPy,y_0} |
| _iteration | {;iteration loop} |
| | {;increment iteration counter} |
| | {let it_no,it_no+1} |
| | {;reset control point counter} |
| | {let cp_no,0} |
| | {;control points, loop until done} |
| | {_conpt} |
| | {;matrix calculations} |
| | {;find D transpose} |
| | {BlockTranspose D_matrix,D_trans} |
| | {;calc DtXL} |
| | {multiply.matrix_1 D_trans} |
| | {multiply.matrix_2 L_matrix} |
| | {multiply.destination DtXL} |
| | {multiply.go} |
| | {;calc DtXD} |
| | {multiply.matrix_1 D_trans} |
| | {multiply.matrix_2 D_matrix} |
| | {multiply.destination DtXD} |
| | {multiply.go} |
| | {;calc DtXD inverse} |
| | {invert.source DtXD} |
| | {invert.destination DtXD1} |
| | {invert.go} |
| | {;now calc diffs.} |
| | {multiply.matrix_1 DtXD1} |
| | {multiply.matrix_2 DtXL} |
| | {multiply.destination diffs} |
| | {multiply.go} |
| | {;apply diffs to estimated values} |
| | {let omega,omega+dodeg} |
| | {let phi, phi+dpdeg} |
| | {let kappa,kappa+dkdeg} |
| | {let XC,XC+dXC} |
| | {let YC,YC+dYC} |
| | {let ZC,ZC+dZC} |
| | {let foc,foc+df} |
| | {let PPx,PPx+dx_0} |
| | {let PPy,PPy+dy_0} |
| | {;test solution} |
| | {IF maxtst=1}{quit} |

| Name | Code |
|---|---|
| | {IF it_no>=imax}{quit} |
| | {branch _iteration} |
| | {quit} |
| | |
| _conpt | {;control point calculations} |
| | {;increment cp counter} |
| | {let cp_no,cp_no+1} |
| | {;get control pt. measured values} |
| | {IF cp_no=1}{blockcopy cpA,xp} |
| | {IF cp_no=2}{blockcopy cpB,xp} |
| | {IF cp_no=3}{blockcopy cpC,xp} |
| | {IF cp_no=4}{blockcopy cpD,xp} |
| | {IF cp_no=5}{blockcopy cpE,xp} |
| | {IF cp_no=6}{blockcopy cpF,xp} |
| | {IF cp_no=7}{blockcopy cpG,xp} |
| | {IF cp_no=8}{blockcopy cpH,xp} |
| | {IF cp_no=9}{blockcopy cpI,xp} |
| | {IF cp_no=10}{blockcopy cpJ,xp} |
| | {IF cp_no=11}{blockcopy cpK,xp} |
| | {IF cp_no=12}{blockcopy cpL,xp} |
| | {_fillD} |
| | {_fillDiff} |
| | {IF cp_no<nocp}{Branch _conpt} |
| | {return} |
| | |
| _fillD | {;place d coeff's in D Matrix} |
| | {put D_matrix,0,(cp_no-1)*2,d_11} |
| | {put D_matrix,1,(cp_no-1)*2,d_12} |
| | {put D_matrix,2,(cp_no-1)*2,d_13} |
| | {put D_matrix,3,(cp_no-1)*2,d_14} |
| | {put D_matrix,4,(cp_no-1)*2,d_15} |
| | {put D_matrix,5,(cp_no-1)*2,d_16} |
| | {IF nounk=6}{branch _endfl1} |
| | {put D_matrix,6,(cp_no-1)*2,d_17} |
| | {put D_matrix,7,(cp_no-1)*2,d_18} |
| | {put D_matrix,8,(cp_no-1)*2,d_19} |
| _endfl1 | {put D_matrix,0,(cp_no-1)*2+1,d_21} |
| | {put D_matrix,1,(cp_no-1)*2+1,d_22} |
| | {put D_matrix,2,(cp_no-1)*2+1,d_23} |
| | {put D_matrix,3,(cp_no-1)*2+1,d_24} |
| | {put D_matrix,4,(cp_no-1)*2+1,d_25} |
| | {put D_matrix,5,(cp_no-1)*2+1,d_26} |
| | {IF nounk=6}{branch _endfl2} |
| | {put D_matrix,6,(cp_no-1)*2+1,d_27} |
| | {put D_matrix,7,(cp_no-1)*2+1,d_28} |
| | {put D_matrix,8,(cp_no-1)*2+1,d_29} |
| _endfl2 | {return} |
| | |
| _fillDiff | {;place photo coord diffs in matrix} |
| | {put L_matrix,0,(cp_no-1)*2,xp_F} |
| | {put L_matrix,0,(cp_no-1)*2+1,yp_G} |
| | {return} |
| | |
| _sizmat | {;subroutine to size matrices} |
| | {blockname.delete D_matrix} |
| | {blockname.create D_matrix,+@cell("address",D_matrixi)&".."&@indextoletter(@cell("col",D_matrixi)+(nounk- |
| | {blockname.delete L_matrix} |
| | {blockname.create L_matrix,+@cell("address",L_matrixi)&".."&@indextoletter(@cell("col",L_matrixi)- |
| | {blockname.delete D_trans} |
| | {blockname.create D_trans,+@cell("address",D_transi)&".."&@indextoletter(@cell("col",D_transi)+(2*nocp- |
| | {blockname.delete DtXD} |
| | {blockname.create DtXD,+@cell("address",DtXDi)&".."&@indextoletter(@cell("col",DtXDi)+(nounk- |
| | {blockname.delete DtXD1} |
| | {blockname.create DtXD1,+@cell("address",DtXD1i)&".."&@indextoletter(@cell("col",DtXD1i)+(nounk- |
| | {blockname.delete DtXL} |

| Name | Code |
|---|---|
| | {blockname.create DtXL,+@cell("address",DtXLi)&".."&@indextoletter(@cell("col",DtXLi)- |
| | |
| _resid | {;subroutine to calc residuals} |
| | {;calc DXX} |
| | {multiply.matrix_1 D_matrix} |
| | {multiply.matrix_2 diffs} |
| | {multiply.destination DXX} |
| | {multiply.go} |
| | {;copy L_matrix} |
| | {blockcopy L_matrix,L_res} |

# List of Block Names

| Name | Block Address |
|---|---|
| | |
| _conpt | Macros:B71 |
| _fill | Macros:B93 |
| _fillD | Macros:B93 |
| _fillDiff | Macros:B117 |
| _initialize | Macros:B5 |
| _iteration | Macros:B25 |
| _sizmat | Macros:B123 |
| Cont. Pts | Initial:C9..G9 |
| cp_no | ContPt:D4 |
| cpA | Initial:C10..G10 |
| cpB | Initial:C11..G11 |
| cpC | Initial:C12..G12 |
| cpD | Initial:C13..G13 |
| cpE | Initial:C14..G14 |
| cpF | Initial:C15..G15 |
| cpG | Initial:C16..G16 |
| cpH | Initial:C17..G17 |
| cpI | Initial:C18..G18 |
| cpJ | Initial:C19..G19 |
| cpK | Initial:C20..G20 |
| cpL | Initial:C21..G21 |
| d_11 | ContPt:C21 |
| d_12 | ContPt:C22 |
| d_13 | ContPt:C23 |
| d_14 | ContPt:C24 |
| d_15 | ContPt:C25 |
| d_16 | ContPt:C26 |
| d_17 | ContPt:C27 |
| d_18 | ContPt:C28 |
| d_19 | ContPt:C29 |
| d_21 | ContPt:C30 |
| d_22 | ContPt:C31 |
| d_23 | ContPt:C32 |
| d_24 | ContPt:C33 |
| d_25 | ContPt:C34 |
| d_26 | ContPt:C35 |
| d_27 | ContPt:C36 |
| d_28 | ContPt:C37 |
| d_29 | ContPt:C38 |
| D_matrix | Iteration:B29..J42 |
| D_matrixi | Iteration:B29 |
| D_trans | Iteration:B90..O98 |
| D_transi | Iteration:B90 |
| dangle | Initial:C37 |
| dcoord | Initial:C38 |
| df | Iteration:G20 |
| diffs | Iteration:G12..G19 |
| dk | Iteration:G14 |
| dkdeg | Iteration:H14 |
| do | Iteration:G12 |
| dodeg | Iteration:H12 |
| dp | Iteration:G13 |
| dpdeg | Iteration:H13 |
| Dt | Iteration:B90..Y98 |
| DtXD | Iteration:B101..J109 |
| DtXD1 | Iteration:B111..J119 |
| DtXD1i | Iteration:B111 |
| DtXDi | Iteration:B101 |
| DtXL | Iteration:B121..B129 |
| DtXLi | Iteration:B121 |
| DX | ContPt:C7 |
| dx_0 | Iteration:G18 |
| dXC | Iteration:G15 |
| DY | ContPt:C8 |
| dy_0 | Iteration:G19 |
| dYC | Iteration:G16 |
| DZ | ContPt:C9 |
| dZC | Iteration:G17 |
| f_0 | Initial:C32 |
| foc | Iteration:J7 |
| imax | Initial:C41 |
| iofixed? | Initial:F25 |
| it_no | Iteration:C4 |
| kappa | Iteration:C9 |
| kappa0 | Initial:C28 |
| krad | Iteration:D9 |
| L_matrix | Iteration:B63..B76 |
| L_matrixi | Iteration:B63 |
| m_11 | Iteration:C17 |
| m_12 | Iteration:C18 |
| m_13 | Iteration:C19 |
| m_21 | Iteration:C20 |
| m_22 | Iteration:C21 |
| m_23 | Iteration:C22 |
| m_31 | Iteration:C23 |
| m_32 | Iteration:C24 |
| m_33 | Iteration:C25 |
| maxtst | Iteration:G24 |
| nocp | Initial:C22 |
| nounk | Initial:F27 |
| omega | Iteration:C7 |
| omega0 | Initial:C26 |
| orad | Iteration:D7 |
| phi | Iteration:C8 |
| phi0 | Initial:C27 |
| PPx | Iteration:J8 |
| PPy | Iteration:J9 |
| prad | Iteration:D8 |
| q | ContPt:C17 |
| r | ContPt:C15 |
| resids | Residuals:B3..B26 |
| s | ContPt:C16 |
| X | ContPt:H8 |
| x_0 | Initial:C33 |
| XC | Iteration:G7 |
| XC0 | Initial:C29 |
| xp | ContPt:F8 |
| xp_F | ContPt:G21 |
| Y | ContPt:I8 |
| y_0 | Initial:C34 |
| YC | Iteration:G8 |
| YC0 | Initial:C30 |
| yp | ContPt:G8 |
| yp_G | ContPt:G22 |
| Z | ContPt:J8 |
| ZC | Iteration:G9 |
| ZC0 | Initial:C31 |
| YC0 | Initial:C30 |
| YL | Iteration:G8 |
| YL0 | Initial:C30 |
| yp | ContPt:G8 |
| yp_G | ContPt:G22 |
| Z | ContPt:J8 |
| ZC | Iteration:G9 |
| ZC0 | Initial:C31 |
| ZL | Iteration:G9 |
| ZL0 | Initial:C31 |

# APPENDIX D

## FIELD DATA

Date - 7 April 2001
Total Station - Nikon DTM-A20LG, ser. no. 820688
EDM corrections - 12 deg. C, 29.9 in.Hg
Distances in meters, Angles as deg.min.sec

Location of Control Points

| To | Az | Zenith Angle |
|---|---|---|
| | From A (H.I. - 1.395) | |
| B | 00.00.00 | - |
| 1 | 24.06.00 | 88.22.55 |
| 2 | 45.05.35 | 88.25.40 |
| 3 | 41.16.55 | 89.28.30 |
| 5 | 25.22.50 | 93.12.00 |
| 6 | 44.08.45 | 93.04.25 |
| 7 | 41.34.05 | 91.05.15 |
| 9 | 40.30.05 | 90.30.20 |
| | From B (H.I. - 1.385) | |
| A | 00.00.00 | - |
| 1 | 275.57.52 | 106.24.18 |
| 2 | 286.10.27 | 98.51.02 |
| 3 | 236.45.10 | 92.38.40 |
| 4 | 244.06.58 | 92.43.18 |
| 6 | 286.22.42 | 105.14.32 |
| 8 | 243.05.25 | 94.40.50 |
| 9 | | |
| | From C (H.I. - 1.405) | |
| A | 00.00.00 | - |
| 3 | 134.33.35 | 95.22.55 |
| 4 | 144.24.12 | 95.19.55 |
| 7 | 134.49.52 | 97.39.00 |
| 9 | 131.18.22 | 97.40.30 |

Relative locations of Base Points

Total Station at pt. A (H.I. - 1.395)

| To | Tgt hgt | Az | Zenith Angle | Horiz. Dist. |
|---|---|---|---|---|
| B | 1.620 | 359.59.30 | 80.32.25 | 20.494 |
| C | 1.620 | 72.23.25 | 76.54.00 | 22.318 |